EXPERIMENTAL INVESTIGATION OF RECYCLING RARE EARTH ELEMENTS FROM WASTE FLUORESCENT LAMP PHOSPHORS

by

Patrick Max Eduafo

A thesis submitted to the Faculty and the Board of Trustees of the Colorado School of Mines in partial fulfillment of the requirements for the degree of Master of Science (Metallurgical and Material Engineering).

Golden, Colorado

Date:⎯⎯⎯⎯⎯⎯⎯

Signed: ⎯⎯⎯⎯⎯⎯⎯⎯⎯⎯⎯

Patrick Max Eduafo

Signed: ⎯⎯⎯⎯⎯⎯⎯⎯⎯⎯⎯

Dr. Brajendra Mishra

Thesis Advisor

Golden, Colorado

Date:⎯⎯⎯⎯⎯⎯⎯

Signed: ⎯⎯⎯⎯⎯⎯⎯⎯⎯⎯⎯

Dr. Michael Kaufman

Professor and Head

Department of Metallurgical & Material Engineering

ABSTRACT

Characterization techniques and experimental measurements were used to evaluate a process for recycling rare earth elements (REEs) from spent fluorescent lamp phosphors. QEMSCAN analysis revealed that 70% of the rare earth bearing minerals was less than 10 µm in size. Feeds of varying characteristic were received throughout the course of the experimental analysis. A representative sample of the as-received feed contained 5.8% total rare earth elements (TREE) and upon sieving to below 44 µm, the grade increased to 16.5% TREE. By sieving further to below 10 µm, the grade increased to 19.8% TREE.

Hydrochloric acid was used as lixiviant in batch leach experiments on the phosphor powder. The maximum extraction obtained was 90% for europium and yttrium at the following conditions: 1.5 M HCl, 70°C, 1 hr, 30 g/L and 200 rpm. However, the solubility of cerium, lanthanum and terbium remained low under these conditions. Multistage leaching and calcination followed by leaching processes also resulted in poor extraction of cerium, lanthanum and terbium.

Based on experimental results a new process for extracting the chief REEs from end of life fluorescent lamps has been developed. The proposed process employs a multistage acid leach using HCl under both mild and strong leaching conditions in addition to thermal treatment of the powder. Using this process, about 90% of the europium and yttrium is extracted in the first stage leach and over 90% of lanthanum in the second stage leach. There is also over 80% of cerium and terbium extracted which marks a significant improvement.

Precipitation using oxalic acid as precipitant and sodium hydroxide for pH adjustment was able to recover 100% of the REE from the leach liquor. However, the purity of the mixed rare earth oxides produced is very low because of co-precipitation of impurities from the leach liquor. The process needs to be optimized for potential industrial application.

Keywords: Rare earth elements, rare earth oxides, phosphor, fluorescent lamp, recycling, leaching, precipitation, calcination

TABLE OF CONTENTS

LIST OF FIGURES

LIST OF TABLES

ACKNOWLEDGMENTS

PROJECT OVERVIEW

Increasing demands for rare earth elements (REEs) due to rapid technological growths in several high-technology applications such as green energy, defense related applications, efficient fuel vehicles, emissive displays and fluorescent lamps, etc. coupled with shortage of supply has forced a paradigm shift towards finding alternative routes for rare earth production and supply. REEs are never found as free metals in the earth's crust and their naturally occurring minerals consist of mixtures of various REEs and non-metals. Despite their name, they are relatively abundant in the earth's crust but in concentrations too small to make mining economical, so global supply relies on a small number of sources. Currently 95% of the world's rare earth metal mining and oxide production comes from China. However, the Chinese government has implemented new tariffs and mining regulations, which have restricted the trade in the precious commodity.

In order to overcome China's dominance it has become important to recycle rare earths from a myriad of sources including permanent magnets, lamp phosphors, rechargeable Ni-MH batteries and catalysts. Recycling of rare earths from the dust generated during high intensity magnet production has been well researched and the technology is commercially available for industrial application. However, like most other cases, in spite of several successful efforts made to devise a feasible process, none of them have been implemented industrially.

In the case of recycling REEs from waste fluorescent lamps fixtures, considerable improvements need to be made in developing the extractive metallurgy aspect and creating efficient disposal and collection systems so as to operate at volumes that may make the process commercially viable. Phosphor dust is generated from spent fluorescent lamps after the glass has been removed and the mercury retorted.

The goal of this project will be to assess the phosphor dust physically and chemically, and based on the valuable metal content, develop efficient recycling routes.

CHAPTER 1

BACKGROUND

1.1. Rare Earth Elements

The rare earth elements (REEs) are a group of 17 elements which appear in the periodic table. The group consists of the 15 lanthanides chemical elements (atomic number 57 to 71) along with scandium and yttrium (Figure 1.1). Scandium and yttrium are considered rare earth elements since they tend to occur in the same ore deposits as the lanthanides and exhibit similar chemical properties. REEs share many similar properties, which is why they occur together in geological deposits but their distribution and concentrations vary. They were originally obtained as earths or oxides from relatively rare minerals, thus they were named rare earths.

Despite their name, rare earth elements (with the exception of the radioactive promethium) are not rare but relatively plentiful in the earth's crust. The more abundant REE are each similar in crustal concentration to commonplace industrial metals such as chromium, nickel, copper, or lead. Even the least abundant REE, thulium, is nearly 200 times more common than gold. However, in contrast to ordinary base and precious metals, REE have very little tendency to become concentrated in exploitable ore deposits. Therefore they are also referred to as 'rare' because it is not common to find them in commercially viable concentrations.

Figure 1.1: The Rare earth elements are subdivided into LREE and HREE.

REEs are classified into two categories - light rare earth elements (LREEs) and heavy rare earth elements (HREEs) based on their electron configuration (Figure 1.1). The LREEs are defined as lanthanum through gadolinium, atomic number 57 to 64. The HREEs are defined as terbium through lutetium, atomic number 65 to 71, and also yttrium (atomic number 39). All the HREEs have 'paired' electrons whereas the LREEs have unpaired electrons, from 0 to 7. Yttrium is lighter than the light rare earths, but included in the HREEs group because of its similar ionic radius, chemical properties and physical associations with heavy rare earths in natural deposits. Scandium is also trivalent; however, its other properties are not similar enough to classify it as either a LREE or HREE. The HREEs are relatively less common in nature but more valuable. The individual REEs can vary widely in their relative natural abundance, ranging from cerium, the most abundant, to promethium which is virtually unknown in ore deposits because it undergoes radioactive decay. One interesting feature of the lanthanides is that the Oddo-Harkins rule applies to their occurrence in nature, in that the odd-numbered elements occur less extensively than the even-numbered ones. In terms of physical properties, there is a general increase in rare-earth metal hardness, density and melting point from cerium to lutetium. There is also widespread readiness for the metals to oxidize at relatively low temperatures, with ignition in air in the temperature range 150˚C–180˚C [1].

There are about 200 rare earth minerals distributed in a wide variety of mineral classes - oxides, phosphates, carbonates, silicates, halides, etc. [2]. The principal rare-earth ores, the minerals monazite and bastnaesite, have formed the basis for historical production, with minor contributions from deposits containing xenotime, apatite, REE bearing clays, allanite, zircon, euxenite, and loparite [3]. The deposits of these minerals are found primarily in China, United States, India, Brazil, South Africa and Australia. Until the discovery of carbonatite-hosted rare-

earth deposits, such as Mountain Pass in California, all rare-earth production came from monazite, with beach-sand operations in India and Brazil the leading producers. Monazite, a phosphate mineral, is known to exist in at least four forms, depending on whether Ce, La, Nd or Pr is the principal rare earth component. Its main drawback is its thorium content, with concerns over the potential radioactivity of tailings having effectively rendered it unacceptable as a commercial ore in most parts of the world. There was minor monazite production in Brazil in 2004, according to British Geological Survey data, while Indian production has tailed off completely. Malaysian monazite production comes as a by-product of alluvial tin mining [4].

Bastnaesite, a carbonate-fluoride mineral, also has more than one composition, with Ce, La or Y forming the main rare earth constituent. Bastnaesite is typically richer in the light rare-earth metals than is monazite. It is usually hosted in carbonatite deposits and is now the main source of world production. It is also present with monazite at Bayan Obo in China, although this is not a carbonatitetype deposit. Bastnaesite won from Mountain Pass supplied the U.S. market with rare earths for most of the last 60 years, with small-scale production having resumed in 2008 after a six-year hiatus. Since 1985, production of REE in China has increased dramatically and now China controls more than 90% of the global supply of rare-earth minerals [5].

Xenotime is another source of rare earth minerals but only a minor contributor to REEs production. It is also a rare-earth phosphate in which yttrium is the major component; a number of heavy rare earth elements can replace some of the yttrium in the atomic structure, as can thorium and uranium. Virtually the only source of xenotime now is as a by-product from tin-mining in Malaysia. However, a significant proportion of the Chinese rare-earth production is sourced from ion absorption clays, which themselves appear to have been derived from the deep weathering of source rocks containing xenotime [6].

1.2. Short History of Rare Earth Elements

The history of rare earth minerals begins in the year 1751, when the Swedish mineralogist and chemist Axel Fredrik Cronstedt (1722-1765) described an unusually heavy, reddish mineral (later named cerite) which he had found in the quarry of Bastnäs, in Sweden. The famous Swedish chemist Carl Wilhelm Scheele (1742-1786) analyzed it and came to the conclusion that it was only an iron aluminum silicate and the mineral was more or less forgotten for next five decades [7]. The identification of each of the rare earth elements took about 150 years, between 1788 and 1941. K.A. Gschniedner divided the history of rare earth metallurgy into three stages – The Dark Ages (before 1950), The Enlightenment Age (1950-69) and The Golden Age (from 1970).

1.2.1. The Dark Ages

The Dark Ages began with the discovery of Rare earths in the town Yttterby, Sweden in the year 1788. During this period, identification of most of the rare earth bearing elements was completed and independent scientific research in different countries had come up with novel methods to extract rare earth mixtures from the available sources. Mosander prepared a highly impure form of cerium metal by reduction of cerium chloride by sodium or potassium. More studies were conducted to understand the chemical and physical properties of the rare earths [8].

1.2.2. The Age of Enlightenment

Prior to this period, the rare earths obtained were 90-95 % pure. During the Age of Enlightenment, major steps were made into producing high purity rare earth elements. Much work was conducted during this period to establish procedures, which would produce 99% pure

rare earths and by the end of this period, rare earth metals with purity as high as 99.99% were produced. The production of such high purity rare earth elements lead to a better understanding of their properties. It was during this period that Strnat and his research team discovered the superior permanent magnet properties of rare earth and cobalt intermetallic. This development lead to the commercialization of rare earth magnets and created an increased demands for high purity rare earths [9].

Furthermore, during this period the scientific community devised a more concentrated and united effort towards rare earth research. The foundation of the Journal of Less Common Metals in 1959 and the initiation of Rare Earth Research conference in 1960 helped bring the scientific communities across the globe involved in rare earth research together. Another major achievement and progress during the age of enlightenment was the establishment of Rare Earth Information Center in 1966 by the Ames National Laboratory at Iowa State University [10].

1.2.3. The Golden Age

The fundamental and applied research of the previous two ages had laid the foundation that ushered in a new age of rapid progress in the area of rare earth extractive metallurgy and application of rare earths and their alloys in a myriad range of applications. By the Golden age, most of the chemical, electrical and magnetic properties of the rare earths were fully understood. The unsaturated 4f electronic structure of rare earth elements makes them have special properties of luminescence, magnetism and electronics, which could be used to develop many new materials.

These properties have now made rare earth elements critical for a diverse and expanding array of high-technology applications, which constitute an important part of the industrial

economy of the 21st century. As a matter of fact, rare earths have been listed in the category of strategic elements in many countries, such as the USA and Japan. Presently they are used in almost all guided missile systems, unmanned drones, advanced sonar, secure communication systems, advanced jet aircraft engines, advanced armor, advanced radar, stealth technologies and targeting and triggering systems. Additionally, rare earth metals are important alloying addition to steels. They also play a key role in the green energy sector. Electric and hybrid cars can contain 20-25 pounds of rare earths, which is double that found in a standard gasoline vehicle [11]. The battery itself is made from several pounds of rare earth compounds. REEs are also used in regenerative braking systems and electric traction motors. The motors consist of powerful magnets made from neodymium and dysprosium. REEs are also used to make high capacity wind turbines, advanced solar panels, high efficiency lighting, petroleum and pollution control catalysts for automobiles and high speed rails [12].

Rare earths also hold promising potential in refrigeration and cooling applications which can help reduce fossil fuel consumption by 15%. They are also being used extensively in fiber optics, advanced electric motors, lasers and X-ray equipment and common modern gadgets like cellphones, computer hard drives, and color televisions. Europium and yttrium, for example, provides red phosphor for televisions and computer monitors and it has no known substitute. Cerium similarly rules the glass-polishing industry. According to IMCOA (2008), the chief users of rare earth metal by weight are catalysts (68%), ceramics (7%), metal alloys (7%), polishing (5%), glass (5%), magnets (4%) and phosphors (3%) and it is projected by 2014, the major users would be metal alloys (25%), magnets (23%), catalysts (16%), polishing (11%), phosphors (7%) and glass (7%) as shown in Figure 1.2 [13].

These applications of rare earth metals provide opportunities for recycling through strategic end of life management. Many of the applications could provide efficient sources for heavy rare earth elements, which are scarce but critical for development of new technologies. As examples, recycling of compact and linear fluorescent lamps can prove to be a useful source of yttrium, europium and terbium whereas recycling of permanent rare earth magnets used in wind and hydro power generation can become an important secondary source of neodymium, praseodymium, dysprosium and terbium. The elemental content of rare earths in appropriately sized phosphor dust that is generated from spent lamps exceeds 5% by total weight.
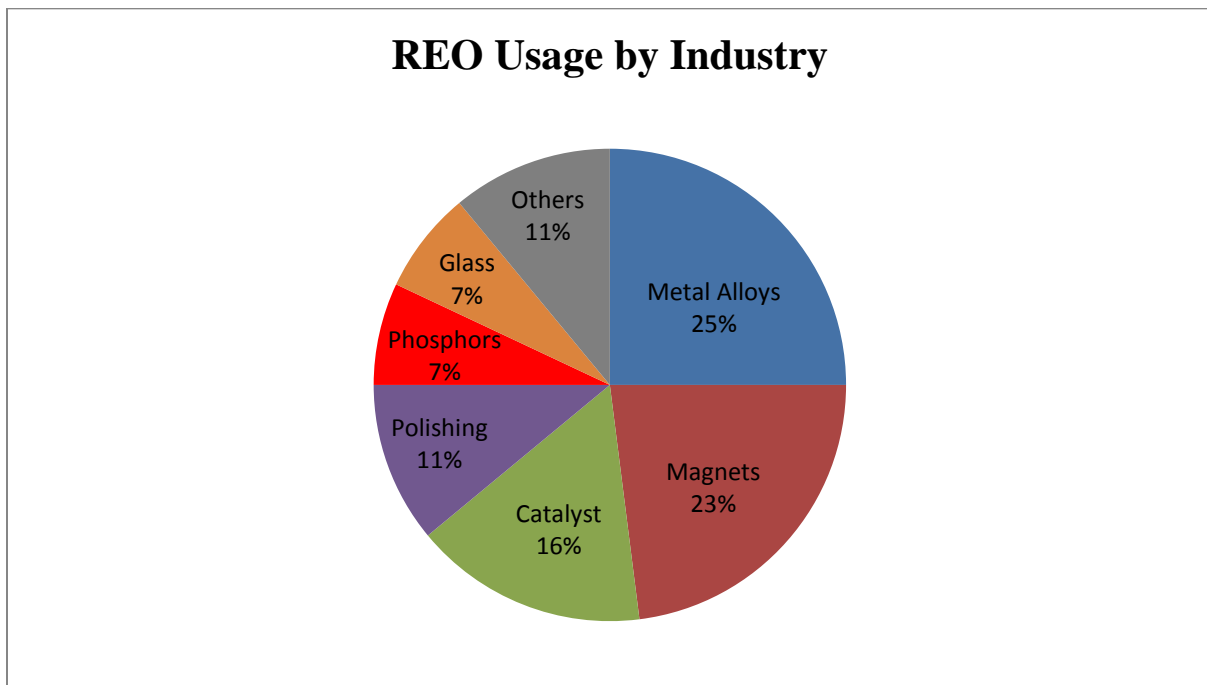
Figure 1.2: Major users of RE metals. Phosphor application is expected to grow.

1.3. Price of REEs

There is a huge demand for rare earth metals in various fast growing sectors: clean energy technologies, colored phosphors, lasers, high intensity magnets, high-tech defense applications and clean energy technologies Therefore to ensure unhindered technological

innovation, it is essential to possess secure supply chains for rare earth elements. Currently, China accounts for 36% of proven world's reserves and dominates as the producer of over 95% of world output of rare earth minerals [14]. The United States continues to be one of the largest consumers and importer of rare earths and the trend is expected to continue as the demand increases. According to a forecast study by IMCOA, the world rare earth demand is projected to rise to 200,000 tons by 2014 and the Chinese production is expected to be around 160,000 tons [15]. Since global demand of REEs exceeded supply due to China's set export quotas, the prices of common metals like Ce, Nd, Sm, La and Y, went up by 150% to 700% within a short period in 2010. The average price of rare earths in 2012 fell close to 40% compared to 2011 and in order to stop the price fall, firms across China adopted strategies such as production suspensions. However, falling demand in downstream sectors and illegal mining curbed the effects of such strategies. Prices have continued to fall in 2013 partly because producers, notably Lynas Corp. of Australia, took measures to increase extraction and processing, diminishing China's influence on pricing (Table 1.1). However, analysts expect prices to rise gradually in the coming months in tandem with demand, and as labor and environmental costs increase.

1.4. REEs as Critical Materials

In recent years REEs have become strategically critical for both developed and developing economies around the world primarily due to the shortage of discovered minable resources (US Congressional Research Service). These developments led to the enactment of the Rare Earths and Critical Material Revitalization Act of 2010 which aims to establish an R&D program within the U.S. Department of Energy (DOE) to ensure long term supply of rare earth materials. In order to ensure secure rare earth supply and attenuate supply-demand imbalance

post 2014, it is imperative to encourage and support exploration of newer REE reserves, build a rare earth stockpile, challenge China on its export policy and also research recycling and reuse of REEs from secondary sources [16].

Table 1.1: Average prices for a standard 99% purity of individual rare earth oxides.

Rare Earths Prices (US$/kg)						
Rare Earths Oxide	**Freight On Board (FOB) China Average Price***					
	2009	**2010**	**2011**	**2012**	**Q1/2013**	**Q2/2013**
Lanthanum Oxide	4.88	22.40	104.10	25.20	11.00	8.42
Cerium Oxide	3.88	21.60	102.00	24.70	11.85	8.49
Neodymium Oxide	19.12	49.50	234.40	123.20	79.15	65.71
Praseodymium Oxide	18.03	48.00	197.30	121.00	85.00	77.64
Samarium Oxide	3.40	14.40	103.40	64.30	25.00	19.36
Dysprosium Oxide	115.67	231.60	1449.80	1035.60	630.00	561.43
Europium Oxide	492.92	559.80	2842.90	2484.80	1600.00	1110.71
Terbium Oxide	361.67	557.80	2334.20	2030.80	1300.00	954.29

Source: Metal Pages

According to the U.S. Department of Energy, some of REEs are on the critical material list (Figure 1.3). The criticality of each element depends on the end application demand pattern. The most critical elements were identified to be neodymium, dysprosium, europium, yttrium and terbium - which are known as the heavy rare earth elements in exception of europium [17]. These minerals, with the exception of yttrium are expected to be in short supply over the next 10-

20 years. The magnitude and duration of these shortages will mainly depend on the success of REE exploration projects. Therefore various governments and industrial users worldwide have begun to develop strategies to safeguard their REE supplies in order to overcome future supply problems. The rising price of many rare earth metals and their criticality as assessed by DOE has now made recycling feasible and attractive.
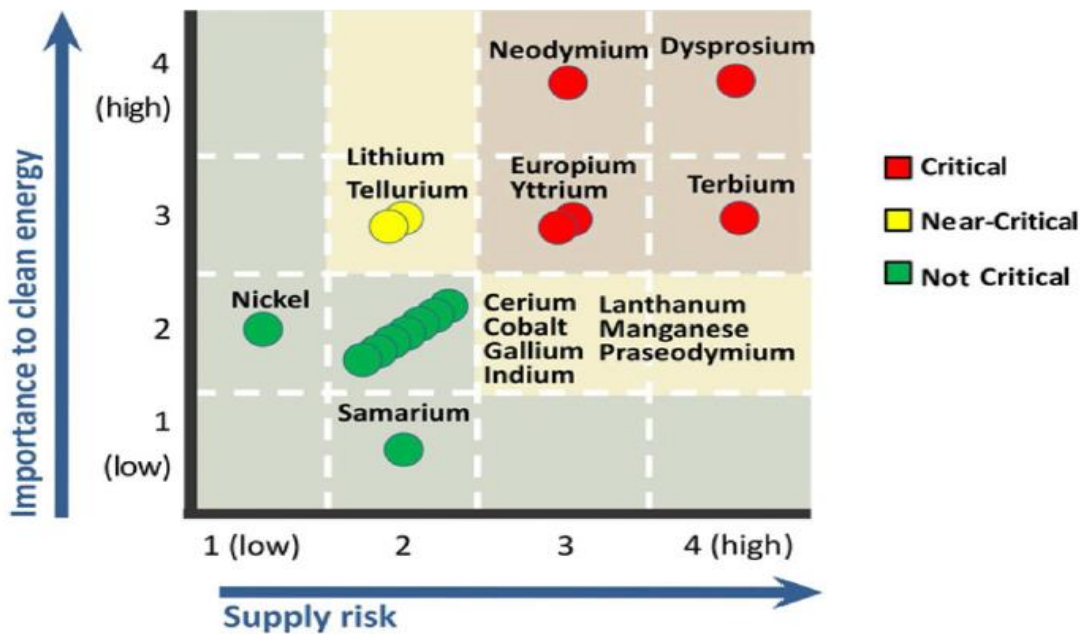
Figure 1.3: Medium term criticality of REEs.

The NSF Center for Resource Recovery and Recycling (CR^3) also initiated a research program for developing technologies to recycle rare earth from phosphor dust which is being carried out at the Colorado School of Mines in partnership with the Worcester Polytechnic Institute. It is anticipated that new projects will be added to look at other waste forms containing rare-earth metals and compounds. Presently, Global Tungsten and Powders Corporation is recycling rare earth from end of life fluorescent lamps commercially. Ellis, Schmidt and Jones [18], have reported that recycling of rare earth based materials would have a stabilizing effect on price, supply, and quality. Currently, potential recyclers do not have a large bank of technologies

to use when considering recycling waste containing rare earth materials. In addition, there is limited infrastructure for the recycling of rare earth based materials. As a result, there is growing interest in recycling REEs from permanent magnets, lamp phosphors, rechargeable Ni-MH batteries and catalysts.

Extensive research on recycling of rare earths from magnets has been done. Zhong et. al. (2010) suggested that 20-30% REE magnets are scrapped during manufacturing stage [19]. Other researchers have suggested various pyrometallurgical and hydrometallurgical routes to recover REE from these scrapped magnets [20]. Efforts have also been made to recover REE from used Ni-MH batteries. During pyrometallurgical treatment of these batteries the REEs report to the slag. Various hydrometallurgical routes have been investigated to recover these elements by Linyan (2009) [21], Bertuol (2009) [22] and Zhang (1999) [23]. There hasn't been much work done in recycling rare earths from catalysts. This may be because catalysts primarily contain low value light rare earths like lanthanum and cerium. However, when the economics of recycling of REE from spent catalysts becomes favorable due to changes in demand, one would expect to recover these light rare earth elements feasibly.

Recycling of rare earths from phosphors provides an efficient way to recover high value heavy rare earth elements. Mei et. al. (2007) has provided an overview of various possible recycling methods for recovery of rare earths from fluorescent powder [24]. A comprehensive literature survey shows the extraction of REEs from their mineral deposits (monazite and bastnaesite) in terms of physical beneficiation of the ore, chemical treatment with acidic or basic solutions, solvent extraction or ion exchange and reduction and refining are well studied and documented. Several flow sheets for processing of REEs from their mineral deposits have been developed and used in commercial operations across the world. Some of the flowsheets have

been modified and applied to the recycling of REEs from spent florescent lamps. The treatment of the phosphors is similar to the ones used for the processing of REE ores.

1.5. Phosphors from Waste Florescent Lamps Fixtures

REEs are used to make phosphors which are widely used for general illumination (fluorescent lamps) and displays (cathode ray tube, backlights for liquid crystal displays, and plasma display panels). Research on the recycling of rare earths from lamp phosphors is restricted to large fluorescent lamps and compact fluorescent lamps with only few studies currently been carried out yet on the recovery of rare earths from small fluorescent lamps used in LCD backlights or from phosphors used in white LEDs [25]. End of life fluorescent lamps are a rich source of cerium, europium, and terbium, which are optically active because of the presence of 4f electrons, and yttrium and lanthanum that are optically inactive due to the absence of 4f electrons.

There are five main rare-earth phosphors found in florescent lamps: the red phosphor Y_2O_3:Eu^{3+} (YOX), the green phosphors $LaPO_4$:Ce^{3+},Tb^{3+} (LAP), $(Gd,Mg)B_5O_{12}$:Ce^{3+},Tb^{3+} (CBT), $(Ce,Tb)MgAl_{11}O_{19}$ (CAT) and the blue phosphor $BaMgAl_{11}O_{17}$:Eu^{2+} (BAM)^{CR}. Lamps produced by non-Chinese manufacturers can contain over 50% wt% halophosphate phosphor $(Sr,Ca)_{10}(PO_4)(Cl,F)_2$:$Sb^{3+}$,$Mn^{2+}$, which is a broadband white emitter. This halophosphate phosphor doesn't contain any REEs and is mixed with YOX to obtain good color-rendering. Among the individual phosphors used in the lamp, YOX has the highest intrinsic value, because it contains large concentrations of yttrium and europium (up to about 20 wt%). In lamps with trichromatic phosphors, the concentration of rare-earth oxides can be as high as 27.9 wt% [26]. The recycled lamp phosphors also contain significant amounts of alumina (Al_2O_3) and silica

14

(SiO_2) that is used in the barrier layer between the phosphor layer and the glass tube to protect the glass envelope against attack by mercury vapor, and thus prevent mercury depletion and reduction of the lamp lumen output. The barrier layer also improves the efficiency of the lamp by reflecting back the UV light that passes through the phosphor layer to the glass layer [27].

Phosphor dust is generated from fluorescent light bulb wastes after the glass and mercury have been removed. Veolia Environmental Services recycles about 27 million lamps per year that produce 1.2 million pounds of phosphor powder per year. Only 30% of the lamps sold per year are recycled (2400 tons per year of phosphor powder). The total market for phosphor dust in US is currently 8000 tons per year and is likely to grow significantly as fluorescent lamp fixtures will replace the incandescent light bulbs. The dust contains economically recoverable amounts of rare earth metal oxides (REO), estimated at 9.0 to 12.5% of phosphor powder. 7% of the REO demand will be in this application of fluorescent light bulbs and tubes. REE recovery technologies can be divided into three general categories: concentration of metal by physical beneficiation, hydrometallurgical leaching and precipitation as well as potential electrometallurgical/pyrometallurgical processing.

1.6. Multistep Method for Recycling REEs from Lamps

The lamps are collected after their end-of-life and processed by specialized companies to recycle glass, metal (filaments, supply electrodes, caps), plastics (caps, insulators), phosphor powder and mercury. Clean glass can be used for the production of new lamps or new glass products while the metal parts are sent to metal recycling facilities and the plastic parts are burnt for energy recovery [28]. The process for recovering REEs from spent florescent lamps include dismantling the lamps mechanically to separate coarse parts, physical and chemical separation

15

methods to remove the phosphor, mercury retort at 345°C to recover the mercury from the phosphor, hydrometallurgical and pyrometallurgical methods to extract the REEs and recovering them as mixed oxides (Figure 1.4). The final step is treatment of the mixed REOs to produce high pure individual REOs.
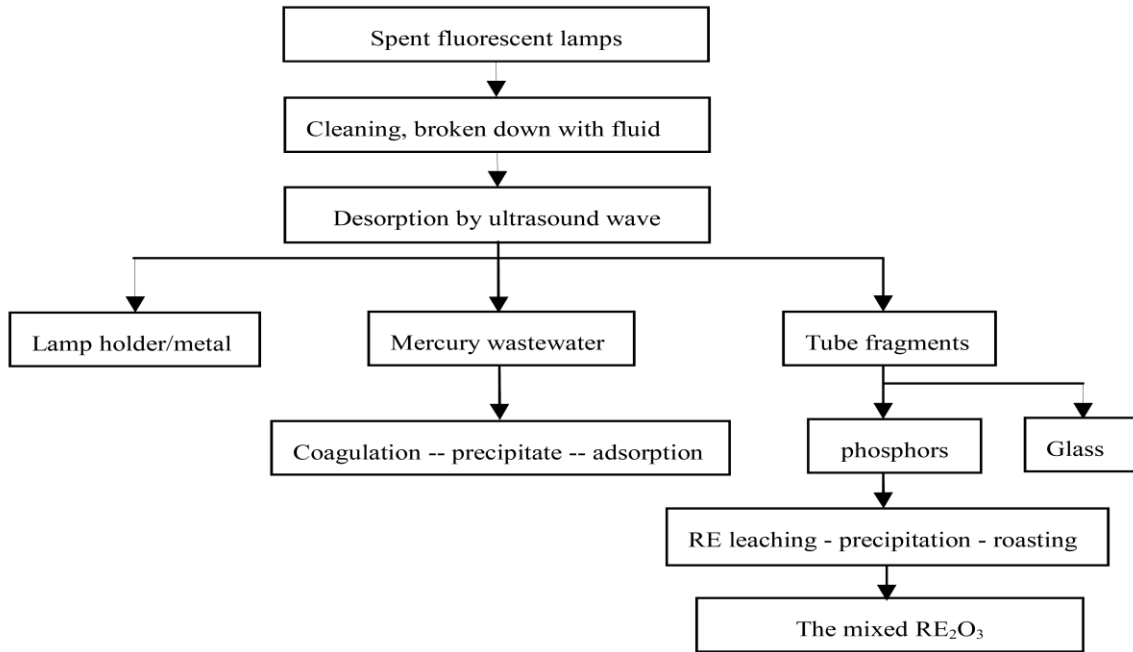
Figure 1.4: Flowchart of the REE separation process.

1.6.1. Physical Beneficiation

Various methods are being used for the recycling of the different materials fractions of the spent fluorescent lamps. Straight-tube lamps are relatively easy to remove their phosphor air-blowing after cutting off both ends ("end cut" method). However, most of such phosphors are of the halophosphate type, and there have limited amounts of the rare earth trichromatic phosphors (red, green, and blue). Recycling of other shapes of lamps and especially the compact fluorescent lamps (CFLs) which contain significant amount of the RE trichromatic phosphor is more problematic.

Most of these used lamps are crushed and shredded to recover glass cullet, aluminum/metal materials, phosphor powder, and mercury. The broken glass pieces are separated from the phosphor powder by a wet or dry sieving operation although it is impossible to remove the very fine glass particles. The lamp phosphor fraction can contain up to 50 wt% of glass and constitutes about 3% of the mass of a fluorescent lamp. This glass fraction lowers the intrinsic value of the lamp phosphors, because it dilutes the REEs content and contaminates the feed solutions of separation plant with silicon during REEs extraction at high temperatures [29]. The lamp phosphor fractions can also be contaminated by zinc sulfide phosphors from cathode ray tubes (CRTs) of old color television sets and computer monitors. The zinc sulfide contamination causes problems when the phosphor fractions are dissolved in acids, because highly toxic hydrogen sulfide gas is formed [30].

Depending on the sources of the lamp phosphors, the recycled lamp phosphor fraction contains mainly six rare earth elements: Y, Eu, La, Ce and Tb. The other REEs are largely absent or present in trace amounts. In addition many non-REE elements are present: Ca, P, Si, P in relatively large concentrations, and Ba, Sr, Mg, Mn, Sb, Cl, F, Hg, Pb, Cd in small to trace concentrations. Fe is largely absent in the lamp phosphor fraction but some amount is introduced into the feed during crushing and milling of the lamps.

Electrostatic separation for physical beneficiation of lamp phosphor has been tested. The results were poor primarily due to dusting of powders during the test [31].

1.6.2. Separation of Phosphor Powder Mixtures

The separation of lamp phosphors particles by flotation (froth flotation) is possible although not as easy as separation of mineral ore particles, because all phosphor components are

phosphates, oxides, aluminates or borates and thus rather similar in hydrophobicity, and also because the phosphor particles sizes (5-10 μm) are much smaller than typical mineral particle sizes (~50 μm). Hirajima and co-workers have investigated the feasibility to separate lamp phosphors by flotation using dodecyl ammonium acetate, sodium dodecyl sulfate and sodium oleate as collectors at different pH values [32]. The influence of the dispersant sodium metasilicate was also investigated. No conditions could be found to separate the different rare earth phosphors. Flotation experiments have also been conducted on a phosphor dust of particle size < 75 μm and a total rare earth element (TREE) content of 10.2% using the Denver flotation cell and Cytec's reagent, AERO 6493 to float apatite from silica in the powder. The rougher float grade increased slightly to 11.3% TREE content and the grade further increased to 14.5% after the cleaner flotation. The insignificant grade improvement indicates poor selectivity of the collector for REE bearing minerals [33].

Two-liquid flotation is more suitable than (froth) flotation for the separation of fine particles (< 10 μm) and thus effective for the separation of lamp phosphor particles. The flotation medium consists of a polar solvent (e.g. water or DMF) and a non-polar solvent (e.g. hexane, heptane, octane, nonane) that form two separate phases. The wettability of the particles can be manipulated by means of a surfactant. Separation is achieved by shaking the powder mixture with a mixture of the two immiscible solvents, with a surfactant dissolved in the non-polar solvent. After agitation, the mixture is allowed to settle. One component of the mixture migrates toward the non-polar phase and remains at the interface of two phases, whereas the other component (or a mixture of components) remains in the polar phase [34]. Thus a mixture of red phosphor $Y_2O_3:Eu^{3+}$, green phosphor $LaPO_4:Ce^{3+},Tb^{3+}$ and $(Sr,Ca,Ba,Mg)_5(PO_4)_3Cl: Eu^{2+}$, a less common blue phosphor, could be separated by a two-step two-liquid flotation process, using

N,N-dimethylformamide (DMF) as the polar phase and heptane as non-polar phase. The green phosphor can be collected at the interface in the first step using dodecyl ammonium acetate as surfactant, and the blue phosphor collected at the interface with sodium 1-octanesulfonate as surfactant, while the red phosphor remained in the DMF phase thereby achieving over 90% recovery and purity for each phosphor [35],[36].

Pneumatic separation of a mixture of lamp phosphor particles in an air stream gave only moderate results, because the differences in particle size have a more pronounced effect on the separation than differences in density between the particles: small heavy particles can settle at the same speed as large light particles [37]. A mixture of phosphor particles has been separated in a dense medium (diiodomethane, $\rho = 3.3$ g/cm^3) [38]. The separation of the fine phosphor particles was accelerated by centrifugation and pretreatment of the particles with sodium oleate improved the separation efficiency. However, process has high cost and the toxicity of diidomethane is a problem. It has been proposed to separate the individual phosphors in a mixture by a method based on differences in magnetic susceptibility [39]. Phosphors with a high terbium content such as $LaPO_4:Ce^{3+},Tb^{3+}$, $(Gd,Mg)B_5O_{12}:Ce^{3+},Tb^{3+}$ and $(Ce,Tb)MgAl_{11}O_{19}$ are substantially more paramagnetic with respect to the europium-based phosphors or the halophosphate phosphors, and thus they are more strongly attracted towards magnetic fields [40].

1.6.3. Extraction of REEs from reclaimed lamp phosphors

The reclaimed lamp phosphor mixtures are a rich source of REEs, especially the heavy REEs such as yttrium, europium and terbium. However, there is quite a significant loss during phosphor recycling. The concentration of rare-earth oxides in lamps with trichromatic phosphors can be as high as 27.9 wt%, but the actual recycled phosphor fractions contain about 10 wt% of

rare earths oxides [41]. In order to recover the rare-earth values, the phosphor mixture has to be chemically attacked to bring the REEs into solution and recovered by precipitation or solvent extraction. Yttrium and europium exist as oxides in the phosphor whereas cerium, lanthanum and terbium occur as phosphates. Therefore the resistance of the different phosphor components towards chemical attack by acids and other chemicals varies widely. For example the halophosphate phosphors and Y_2O_3:Eu^{3+} readily dissolves in diluted acids but the rare earth phosphate phosphor $LaPO_4$:Ce^{3+},Tb^{3+} (LAP) and the aluminate phosphors (Ce,Tb)$MgAl_{11}O_{19}$ (CAT) and $BaMgAl_{10}O_{17}$:Eu^{2+} (BAM) are much more resistant toward attack by acids and difficult to dissolve. Dissolution of LAP can be achieved by using the same methods for processing of monazite ore, (Ce,La)PO_4 [42].

Takahashi's group carried out a series of studies on the hydrometallurgical separation and recovery of rare earths from phosphors in the fluorescent lamp wastes [43], [44], [45]. Sulfuric acid leaching from the rare-earth components was studied under different conditions [46]. After optimization of the leaching conditions, 92% of yttrium and 98% of europium were dissolved at sulfuric acid concentration of 1.5 kmol/m^3, temperature of 70°C, leaching time of 1 h, and pulp concentration of 30 kg/m^3. However there was poor dissolution of cerium, lanthanum and terbium. Wang et al. (2011) have conducted leaching experiments on trichromatic phosphor mixtures and have shown that hydrochloric acid (4 mol L^{-1}) in combination with hydrogen peroxide (4.4 g L^{-1}) is a strong leachant [47]. Rabah proposed a process for the recovery of europium, yttrium and some valuable salts from spent fluorescent lamps by pressure leaching with a H_2SO_4/HNO_3 mixture at 125 °C and 5 MPa for 4 hours and dissolved 92.8% of the europium and 96.4% of the yttrium present in the mixture [48]. Radeke et al. (1998) studied the separation of mercury, calcium, yttrium, and heavy rare earths in disposed fluorescent tubes

containing both halophosphate and trichromatic phosphors [49]. De Michelis et al. (2011) carried out leaching tests on phosphor powders with different acids (HCl, HNO_3, H_2SO_4) and ammonia to find the conditions for the most efficient recovery of yttrium [50]. Leaching with ammonia gave very low yttrium recovery, whereas leaching with nitric acid brought the largest quantities of yttrium into solution, although toxic vapors were formed, and leaching with hydrochloric and sulfuric acid gave similar results. They concluded that leaching with sulfuric acid is to be preferred, since it leads to less co-dissolution of calcium, lead and barium. OSRAM has developed a process to recover all REEs from spent phosphors [51]. The individual process steps are: mechanical separation of coarse parts, separation of the halophosphates, extraction of RE fluorescent materials readily dissolved (Y, Eu oxide), extraction of RE fluorescent materials insoluble in acids (RE phosphates), digestion of the remaining components containing RE (RE aluminates), RE precipitation and final treatment to produce new fluorescent material. Rhodia (Solvay Group) has developed a flow sheet for the recovery of REEs from a mixture of halophosphate and rare-earth phosphors [52]. The phosphors are attacked by hot nitric acid (or hydrochloric acid), and finally by a hot concentrated sodium hydroxide solution or by molten sodium carbonate. The rare earths are recovered from the leach solutions for further separation into the individual elements by a solvent extraction process. Global Tungsten and Powders Corporation also has a commercial operation for recycling rare earth from end of life fluorescent lamps in the USA.

LAP, BAM and CAT phosphors can be chemically attacked by heating them in molten sodium carbonate at 1000˚C [53]. YOX dissolves more readily in acids after a mechanochemical treatment using ball milling [54]. The mechanochemical treatment causes disordering of the crystal structures of the phosphor and this allows dissolution under mild conditions. Yttrium, europium, terbium, lanthanum, and cerium were dissolved in 1 kmol/m^3 HCl at room

temperature after the mechanochemical treatment for 2 hours with more than 80% efficiency [55]. Shimizu et al. (2005) have worked on recovering of REEs from lamp phosphors by extraction with supercritical carbon dioxide containing tri-n-butyl phosphate (TBP) complexes of nitric acid and water [56]. Over 99.5% of the yttrium and europium present in the phosphor mixture was extracted after leaching for 2 hours at 60˚C and 15 MPa. However, control experiments with TBP/HNO_3/H_2O at atmospheric pressure could only extract less than 40% of yttrium and europium.

Yang and co-workers showed that salting-out agents increase the efficiency of a solvent extraction process. They found out that the large amount of Al_2O_3 present in the phosphor mixture (from the barrier layer) is an advantage if the phosphors are dissolved in nitric acid, because the $Al(NO_3)_3$ that is formed can act as a salting-out agent for the extraction of rare earths from the aqueous phase to an organic phase by solvent extraction [57].

1.6.4. Separation by Solvent Extraction and Ion Exchange

Separation of REEs is very difficult due to the small difference in ionic radius, the preference for interaction with hard-sphere base donor atoms and the dominance of the trivalent oxidation state across the lanthanide series [58]. Methods such as fractional crystallization or precipitation, ion-exchange, selective oxidation/reduction and solvent extraction were developed for individual separation of REEs. Fractional crystallization and fractional precipitation are slow and tedious methods that were used in the past and have been replaced by solvent extraction and ion exchange. Solvent extraction and ion exchange separations are based on the lanthanide contraction – the decrease in ionic radius across the lanthanide series of elements, from lanthanum to lutetium [59]. Therefore, heavy members of the series will create stronger bounds

with solute and solvent molecules compared to light members [60], and this allows preferential binding to ion exchange resins, or extraction of the complex into the organic phase [61]. In order to obtain pure rare earth metals (REM), solvent extraction can be used followed by the precipitation of the metals and calcination of the precipitate. Di-(2-ethylhexyl) phosphoric acid (DEHPA) can be used as an extractant for yttrium leaving europium in the raffinate, which can be further removed through selective precipitation or by solvent extraction.

Takahashi et al. (1996) have studied the separation of rare earths in phosphor wastes by chelating resins after a two-step leaching process. Iminodiacetic acid and nitrilotriacetic acid-type resins were used for the mutual separation of the (Y, Eu) and (La, Ce, Tb) fractions, respectively. After oxalate precipitation and calcination, each rare-earth oxides were obtained with the yields as follows: of 50% Y (99.8% purity), 50% Eu (98.3% purity), 30% La and (96.0% purity), 30% Ce and (87.3% purity), and 90% Tb (91.8% purity) [62]. They applied solvent extraction with 2-ethylhehyl phosphonic acid mono-2-ethylhehyl ester (PC-88A) in kerosene to achieve separation between yttrium and europium from the (Y, Eu) fraction. Mutual separation was achieved by the combination of countercurrent 6-stage extraction and 4-stage stripping using small-scale mixer settlers. The purities of yttrium and europium in the obtained oxides were, respectively, 99.3% and 97% with a total rare-earths yield of 65% [63]. They also studied the solvent extraction separation of yttrium and europium from the same leach liquor without precipitation step; that is, yttrium was initially extracted at pH 1.5 and then europium was extracted at pH 2.0 which allowed the extraction of impurities. They obtained the purities of 99.7% for Y_2O_3 and 90% for Eu_2O_3 [64].

Nakamura et al. (2007) studied the solvent extraction separation of rare earths and alkali earths using 2-ethylhehyl phosphonic acid mono-2-ethylhehyl ester (PC-88A) in kerosene using

the leaching solution of phosphor wastes according to Figure 1.5 [65]. Extraction equilibrium

constant for each element was initially obtained assuming the stoichiometries for trivalent rare-

earth ions (and Al^{3+}) and for alkali-earth ions (M^{2+}) as shown in the equation:

$$M^{2+} + 3H_2L_{2org} = M(HL_2)_2(H_2L_2)_{org} + 2H^+$$

They then simulated the extraction and scrubbing behavior from the leaching solution of

phosphor waste by the equilibrium model for the multicomponent and multistage system. They

focused on the selective recovery of europium, terbium and yttrium and established that the

effective separation and recovery of these rare earth metals (REMs) is possible in two steps, in a

counter-current mixer-settler cascade. Recovery percentages from the leaching solution and the

corresponding metal purities were: 97.8% for yttrium (98.1% purity), 52.8% europium (100%

purity) and 58.1% terbium (85.7% purity).
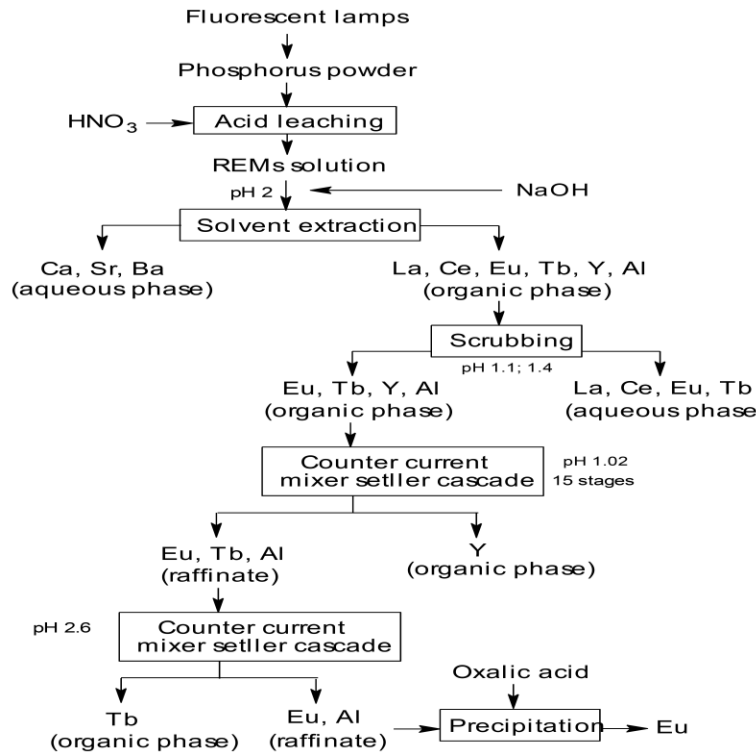
Figure 1.5: Recovery of REMs from phosphor powder using solvent extraction.

Trimethylbenzylammonium chloride has been used to extract the metals from the thiocyanate solution generated after sulfuric acid leach on fluorescent phosphor powder. Maximum extraction was attained at 80°C and extraction percentages of 98.8% (yttrium) and 96.5% (europium) were achieved using a 2:1 solvent:water molar ratio. The metals in the organic phase were recovered as nitrate salts using N-tributylphosphate in nitric acid. Using a 1 M nitric acid at 125°C, a stripping extent of 99% was achieved. The two nitrates were separated by dissolving in ethyl alcohol, in which only yttrium nitrate is soluble. The metals were obtained by thermal reduction using hydrogen at 850°C (for europium) and 1575°C (for yttrium). A metal separation factor of 9.4 was achieved and economic estimations showed that the method can be applied industrially [66].

Mei et al. (2009) has proposed a process to efficiently separate artificial mixtures of red, blue and green phosphors by solvent extraction. 2 thenoyltrifluoroacetone (TTA) dissolved in heptane was used to extract the blue powder at alkaline pH. Potassium sodium tartrate (PST) and Na_2CO_3 were used as regulators. In a second step, chloroform was used to extract the green phosphor into the organic phase, leaving the red phosphor in the aqueous phase. Results of the experiment show that the blue phosphor can be extracted selectively into TTA at pH values from 7 to 11. The blue and green phosphors can be extracted into chloroform, with more than 90% recovery at pH values from 7 to 11, leaving the red phosphor in the aqueous phase. TTA was used to extract the blue phosphor. Extraction of red phosphor from three phosphor mixtures was carried at room temperature and the optimal conditions were found to be: neutral pH, PST concentration from 0.5% to 1.0%, 1-pentanol/chloroform (by volume) in the range of 0.2-0.5%, solid/liquid 5-30 g/L. Regarding grades and recovery of the separated products: red was 96.9% and 95.2%, blue was 82.7% and 98.8%, green was 94.6% and 82.6% [67].

Having been physically beneficiated and chemically treated by means of leaching, ion exchange, solvent extraction and fractional precipitation we obtain rare earth oxides (REOs) which become the natural starting materials to obtain pure metals by means of reduction. REOs are stable oxides and their direct reduction to metal is difficult.

CHAPTER 2

ANALYTICAL TECHNIQUES AND EXPERIMENTAL METHODS

This chapter summarizes the analytical techniques and experimental methods utilized in this project.

2.1. Analytical Techniques

The main analytical techniques utilized in experiments were:

1. Microtrac Particle Size Analyzer

2. QEMSCAN

3. X-Ray Diffraction (XRD)

4. Inductively Coupled Plasma – Atomic Emission Spectroscopy (ICP-AES)

2.1.1. Microtrac Particle Size Analyzer

The Microtrac particle size analyzer gives an accurate understanding of the particle size distribution in samples using the patented tri-laser technology. The system consists of three lasers and two detector arrays that are used to take a measurement of scattered light over a 180-degree spectrum. The resultant scattered light information from all three lasers is combined to generate the particle size distribution. Different samples obtained from Veolia Environmental Services and other sources were analyzed for particle size distribution using a beam with a wavelength of 0.6328 micrometers. Large particles produce a scattered light pattern with low angles and high intensity whereas smaller particles produce wide angles and low intensities.

2.1.2. QEMSCAN

QEMSCAN is an acronym for Quantitative Evaluation of Minerals by Scanning Electron Microscopy. It is a registered trademark owned by the FEI Company. It is configured to measure mineralogical variability based on chemistry at the micrometer-scale. QEMSCAN consists of a base scanning electron microscope, equipped with four light element energy dispersive X-ray detectors, a microanalyser and proprietary software controlling automated data acquisition. QEMSCAN utilizes both the back-scattered electron (BSE) signal intensity as well as an Energy Dispersive X-ray Signal (EDS) at each measurement point to create a mineral composition map. QEMSCAN data includes information on mineral and chemical assay, grain size and shape, mineral association, liberation, porosity, matrix density and elemental deportment. One approximately 1 g split per sample was mixed with epoxy resin in 30 mm molds and left to cure. Sample blocks were ground and polished using water-based lubricants and suspensions finishing with a 1-micron diamond polish. Samples were carbon-coated to establish an electrically conductive surface. QEMSCAN analysis was carried out in Particle Mineral Analysis mode at 3.5-micron resolution using standard operating conditions, i.e. accelerating voltage of 25 kV, specimen current of 5 nA, stage height of 20 mm and a working distance of 22 mm.

2.1.3. X-ray Diffraction

In XRD, X-rays with a relatively low wavelength of up to 0.1 Å, which are comparable to the size of an atom, are used to probe the crystal structure of materials or minerals. The x-rays are produced using X-ray tubes or synchrotron radiations and the interaction of the X-rays with the electrons in the sample generates an analysis of crystal structure as well as the phases present.

When an X-ray beam is made incident on an atom, the constituting x-ray photons may either be deflected elastically without a change in wavelength (Thompson Scattering) or inelastically with a change in wavelength due to loss of energy (Compton Scattering). These diffracted beams interact with each other, which produces a resultant intensity modulation. By measuring the diffraction pattern, the user can evaluate the distribution of atoms in the crystal, as the diffracted beam will contain sharp interference peaks with same symmetry as the atomic distribution. This relationship is governed by Bragg's Law, which establishes a relationship between scattering of an X-ray beam with respect to inter-atomic spacing and the angle of incidence:

$$\lambda = 2\,d\,\sin\theta$$

where 'd' is the inter-atomic distance in the crystal lattice, λ is the X-ray wavelength, and 2θ is the angle between incident and scattered beam. The incident angle and scattered angle are varied throughout the analysis as the X-ray source and detector are rotated about a fixed axis as shown in the Figure 2.1.
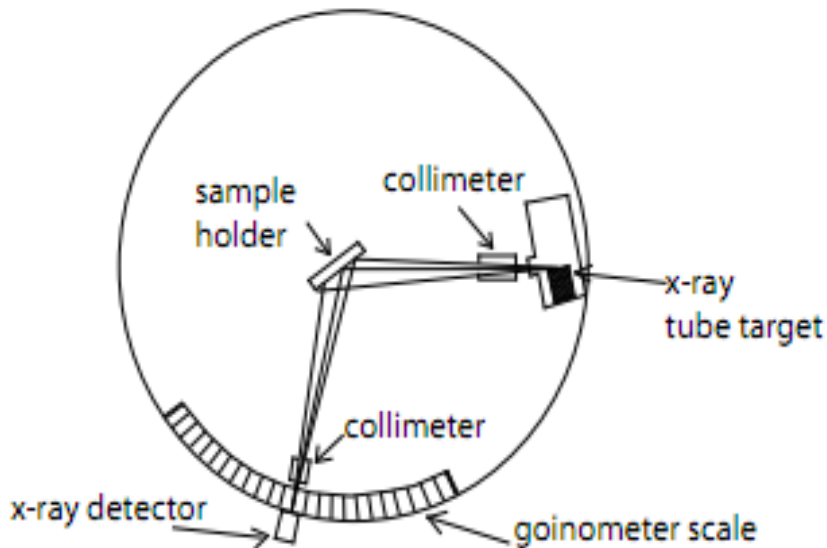
Figure 2.1: A schematic diagram showing the operation of XRD.

Figure 2.2 below shows a photograph of the X-ray diffraction facility available at the Colorado School of Mines (CSM). X-ray diffraction was used to characterize the incoming feed material, the leach residue and the precipitation product.

Figure 2.2: Photograph shows the inside chamber of XRD machine at CSM.

2.1.4. Inductively Coupled Plasma – Atomic Emission Spectroscopy

Inductively Coupled Plasma-Atomic Emission Spectrometry (ICP-AES) is one of the most common techniques for elemental analysis due to its high specificity, multi-element capability and good detection limits. ICP-AES consists of a plasma source, spectrometer and a multi-element detector as shown in Figure 2.3.
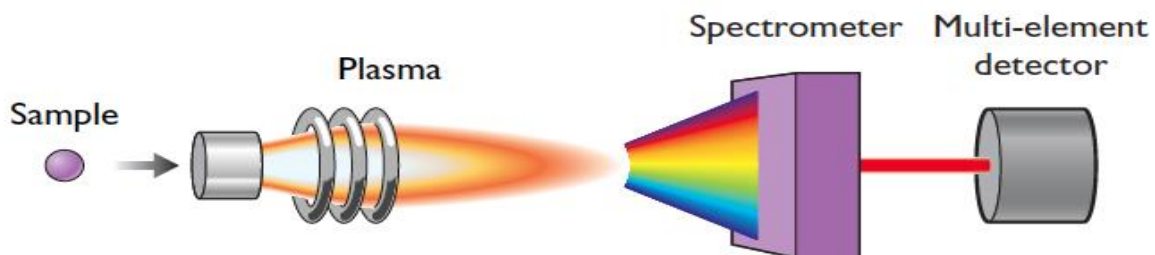
Figure 2.3: Schematic of ICP-AES.

Different kinds of dissolved samples can be analyzed, varying from solutions containing high salt concentrations to diluted acids. The plasma source produces free electrons and highly charged ions (plasma) temperatures in the range of 7,000 K to 10,000 K. The plasma is used to produce strong atomic emission from all elements in the sample by dissociating the sample into its constituent atoms or ions, exciting them to a higher energy level. They return to their ground state by emitting photons of a characteristic wavelength depending on the element present. Each excited element emits specific wavelengths λ, which has a typical emission spectrum. The intensity of the radiation is proportional to the element concentration. The emitted light is recorded by an optical spectrometer, a multi-component part containing mirrors, prism etc. The spectrometer separates the specific wavelengths of interest.

REE have considerably widespread emission spectra within the detection range of ICP-AES. Cerium has more emission lines than any other element, and many of the REE emission lines are closely spaced in the spectral window of ICP-AES leading to considerable interference from the REE on other elements, especially other REE's. Therefore since the atomic emission lines are very narrow lines, a high-resolution detector is essential. Most often a Charge Couple Device (CCD) is used, which provides both high resolution and simultaneous detection which makes it possible to measure all elements of interest at the same time. Simultaneous detection is advantageous because it limits signal variations introduced by sample preparation. When calibrated against standards, ICP-AES provides a quantitative analysis of the original sample.

2.2. Experimental Methods

A brief description of the various experimental methods used in this project is presented in this section.

2.2.1. Dry and Wet Sieving

Based on the QEMSCAN analysis it was understood the rare earth bearing minerals in the feed material were liberated and also 70% of these particles were less than 15 μm. Hence, size based physical beneficiation of the ore was found to be the logical starting point in an effort to further beneficiate the ore in rare earth content.

Wet sieving was done initially to find out the size distribution of the particles in feed material. The method consists of placing the desired sieves in order of decreasing mesh opening and using wash water and a vibrating motor to aid the particles to pass through the mesh. The fraction of feed passing 325 Tyler Mesh, with mesh opening of 44 μm, is used for further leaching experiments. The P_{325} fraction of the samples were also seived to below 10 μm for grade improvement. Dry sieving was employed to sieve the feed material to 44 μm for the leaching and precipitation experiments due to the large sample loss with wet sieving.

2.2.2. Batch Leaching

Batch leaching experiments were conducted to establish operating conditions for the leaching experiments. Based on literature review, HCl, H_2SO_4, HNO_3 and NaOH were used as leaching reagent. The leaching parameters or variables tested were:

1. Acid Concentration

2. Temperature

3. Time

4. Solid to Liquid Ratio (S/L)

5. Agitation speed

The solution was heated to the desired temperature on a hot plate and a magnetic stirrer was added to aid agitation. A weighed sample of the feed material was added to the heated solution and the mixture agitated for desired time. The amount of sample added was governed by the needed solid-liquid ratio. The leached residue was filtered, washed and dried for elemental analysis by ICP-AES.

2.2.3. Precipitation

Preliminary precipitation experiments were conducted at room temperature and pH adjustments were done using sodium hydroxide with oxalic acid as precipitant. A pH meter was used to observe the pH changes. The solution was then stirred for 2 hours to allow time for the rare earth elements to precipitate. The solution was then filtered and the residue (mixed rare earth oxalates) was dried and calcined at 900 ˚C to produce the mixed rare earth oxide powder which was then digested with the lithium borate fusion method before analyzed for the rare earth content with ICP-AES.

2.2.4. Lithium Borate Fusion

Fusion is a method used to solubilize an oxidized sample in a molten flux at temperatures of around 1050˚C - 1100˚C. It does not consist of heating the sample to its melting temperature, but rather having the oxidized samples dissolved into a solvent, generally a lithium borate flux above their melting temperature but not exceed 1050˚C. Thus for optimal dissolution, the right flux composition must be used. Two basic formulations, lithium tetraborate (LiT or $Li_2B_4O_7$, m.p. 920˚C) and lithium metaborate (LiM or $LiBO_2$, m.p. 845˚C) are commonly used in various proportions.

Samples are mixed with 1 g of flux (LiM and LiT, 60:40 wt%) and 2-3 drops of lithium borate (20 mg/L) are added as a non-wetting agent before fused in a Muffle furnace at 1000˚C for 45 minutes. The molten melt is immediately poured into a solution of 5% nitric acid and stirred continuously until completely dissolved (~20 minutes) for ICP-AES analysis.

CHAPTER 3

MATERIAL CHARACTERIZATION AND SIZE BASED SEPARATION

3.1. QEMSCAN Analysis

Waste phosphor dust samples were obtained from different locations for these size based separation. The samples received were labeled PHX, PWG and PWB and were characterized in the previous studies [68]. This data will be edited and presented in this chapter. The samples were quantitatively evaluated for mineralogy and particle size distribution through QEMSCAN. For the sake of brevity, the QEMSCAN and XRD results for PWB and PWG are not shown. The modal mineral abundance in the powder in mass percent is represented below in Figure 3.1.

Figure 3.1: Modal mineral abundance in the PHX powder

The QEMSCAN result shows that the powder consists mainly of broken glass which is obtained from crushing the waste fluorescent lamp tubes. Table 3.1 below also shows the mass distribution of the constituents of the powder. It consists predominantly of a glassy silicate component (68 mass%) in addition to significant amounts of apatite (25 mass%), small quantities of zircon, Ce-phosphate, quartz, and calcite as well as trace amounts of malachite/azurite, cuprite, dolomite, and Fe Oxide/hydroxide. Although the rare earth element abundances are

typically too low to be determined and quantified by QEMSCAN analysis, rare earth element-bearing phases such as apatite, zircon and monazite (Ce-phosphate) can be clearly identified. Zircon and Ce-phosphate can contain relatively high rare earth element abundances. The common impurities in apatite include Ce, La, Eu, Y, Sr, Pr, Er, Nd, Sm, Gd and Dy.

Table 3.1: Mineral distribution in mass % in PHX powder received from Veolia

	PHX
Apatite	25
Zircon	2
Ce-phosphate	1
Malachite/Azurite	tr
Cuprite	tr
Calcite	2
Dolomite	tr
Quartz	1
FeOxide/Hydroxide	tr
Glass	68

*tr = < 0.5 mass %

Assessment of the grain size distribution and mineral associations of the rare earth element-bearing minerals show that they are all less than 30 μm in size with the majority being less than 10 μm (over 70 mass%). All rare earth element-bearing phases appear to be fully liberated. The grain size distribution of the PHX powder is listed in the Table 3.2 below.

Table 3.2: Grain size distribution (in volume %) of rare earth bearing minerals in PHX

	PHX
<5 um	33
<10 um	41
<15 um	20
<20 um	3
<25 um	3
<30 um	0
>30 um	0

3.2. X-ray Diffraction Analysis

X-ray diffraction was carried out to determine the phases of the minerals present in the PHX powder. The major phases identfied were colusite, calcium samarium oxide phosphate and sodium calcium hydrogen phosphate. The strong peaks of sodium calcium hydrogen phosphate are a result of addition of white phosphors which are similar in nature to the apatite phase. The XRD plot for PHX is shown in Figure 3.2 below.
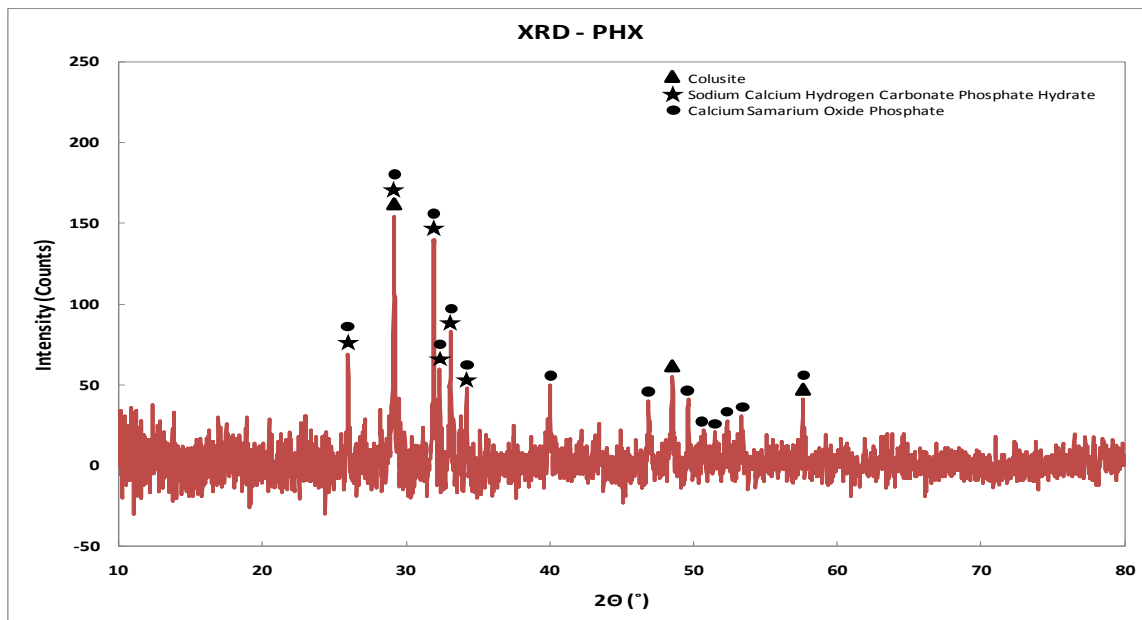
Figure 3.2: XRD plot for phase identification in PHX powder.

3.3. Microtrak Particle Size Analysis

The as-received samples were all analysed for particle size distribution using the microtrak particle size analyser. A comparison of the size distribution of the three samples is shown in Figure 3.3. PHX is seen to have a much finer particle size and has a P_{80} at 45.84 µm where as the P_{80} for PWB and PWG was at 775.3 µm and 303.8 µm respectively.. However, by comparing all the results, it was concluded that the PHX sample has a lot lesser broken glass or

silica content compared to PWB or PWG and thus was chosen for the experimental evaluation of size based separation.
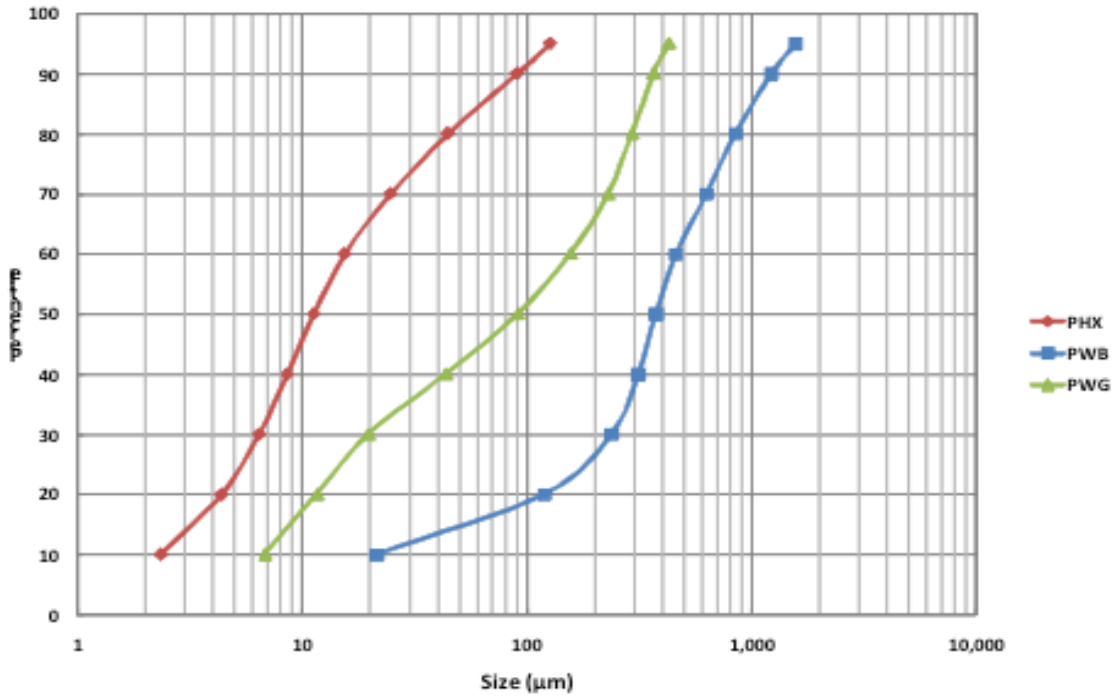
Figure 3.3: Microtrak Particle Size analysis for the three powders.

3.4. Sieving

Wet sieving were employed in the size separation study. The sieving configuration for the wet seiving is shown Figure 3.4. The material was fed onto the 32 Tyler mesh pan and washed with running water. The passing material was collected in a bucket and then transferred over to the 42 Tyler mesh and the sequence following the sieving configuration was repeated till the material was collected in the pan. Based on the wet sieve separation it was again confirmed that both PWG and PWB have much more glass as compared to PHX.

The particle size distribution and cumulative percentage passing value for each of the three powders after the wet sieve is not shown but those results also conclude that all three

powders are similar in constitutent composition but PHX has a relatively lower average particle

size and less silica content.

32
42
60
80
115
170
270
325
400
Pan

Figure 3.4: Seive configuration used for wet seive analysis

The elemental composition of the fraction of PHX Powder pass 325 Tyler Mesh was then analysed using ICP-AES to determine the rare earth content and compared with the rare earth content in the as-received sample. Table 3.3 shows that upon seiving to below 325 Tyler mesh (44 μm), the REE grade of the powder doubles approximately from 2.30% to 4.53%.

Table 3.3: Elemental analysis of the as-received PHX and P_{325} fraction of PHX powder

Rare Earth	As-received PHX (ppm)	% REE	P_{325} of PHX (ppm)	%REE
Ce	3049.21	0.30	5933.01	0.59
Eu	1128.25	0.11	1896.41	0.19
Gd	19.89	0.00	42.18	0.00
La	3572.66	0.36	5497.84	0.55
Lu	2.70	0.00	3.53	0.00
Pr	393.28	0.04	814.52	0.08
Sc	3.08	0.00	39.09	0.00
Sm	82.98	0.01	167.55	0.02
Tb	55.29	0.01	67.78	0.01
Y	14692.48	1.47	30796.05	3.08
Yb	1.13	0.00	1.59	0.00
Total REE*	**23000.95**	**2.30**	**45299.55**	**4.53**

*Dy, Er, Ho, Nd andTm not included in Total REE as they were below betection limit

3.5. Concentration of Rare Earth Elements by Physical Separation

A feasibility study was conducted to concentrate the powder by physical separation. By seiving the the as-received PHX powder to below 44 μm, the grade of the rare earth elements in the powder doubled therefore it was proposed that concentration of the rare earth values could improve by a finer wet sieving. To test this hypothesis new phosphor dust samples were received obtained from Veolia Environmental Services. The new samples were labelled as REP and FLOT and their elemental composition were slightly different from those obtained for PHX as they contained significant amounts of terbium as compared to PHX. REP was a single representative sample from different machines that are used to crush the waste CFLs to obtain the phosphor powder.

After seiving, there was an upgrade of rare earths in both REP and FLOT - 16.50% and 6.68% respectivelty. The P_{325} fraction of REP were seived to below 10 μm for further grade improvement. The percentage passing was 80% and the filtrate was collected in a bucket and dried. Once separated, the P_{10} REP sample was digested using the lithium borate fusion and

analyzed for the total recoverable rare earth elements using ICP-AES. The results from the ICP-AES for these samples are shown in Table 3.4 below and there was grade improvement for each of the individual rare earth elements.

Table 3.4: Elemental analysis of the P_{325} REP and P_{10} fraction of the REP powder.

Rare Earth	% REE	
	P_{325} REP	P_{10} REP
Ce	1.606	1.978
Dy	0.005	0.005
Eu	0.547	0.592
La	4.982	6.972
Nd	0.087	0.104
Pr	0.166	0.208
Tb	0.844	1.052
Tm	0.040	0.041
Y	8.226	8.878
Total REE	**16.503**	**19.834**

The SEM image for the P_{10} fraction shown in Figure 3.5 primarily shows halophosphate and rare earth phases with only secondary silica phases. Total silica content in the as received material and the P_{10} phase needs to be quantified.

However, sieving down to 10 μm is difficult and large amount of liquid filtrate is generated which have to dried by vaccum filtration. Thus although there is a slight upgrade in REE content with fine wet sieving this is countered by inherent operation problems and high cost which will be a major set back for industrial application. Therefore dry sieving to below 44 μm was used for further experimental evaluation of acid and base leach on the powder to extract the rare earth elements.
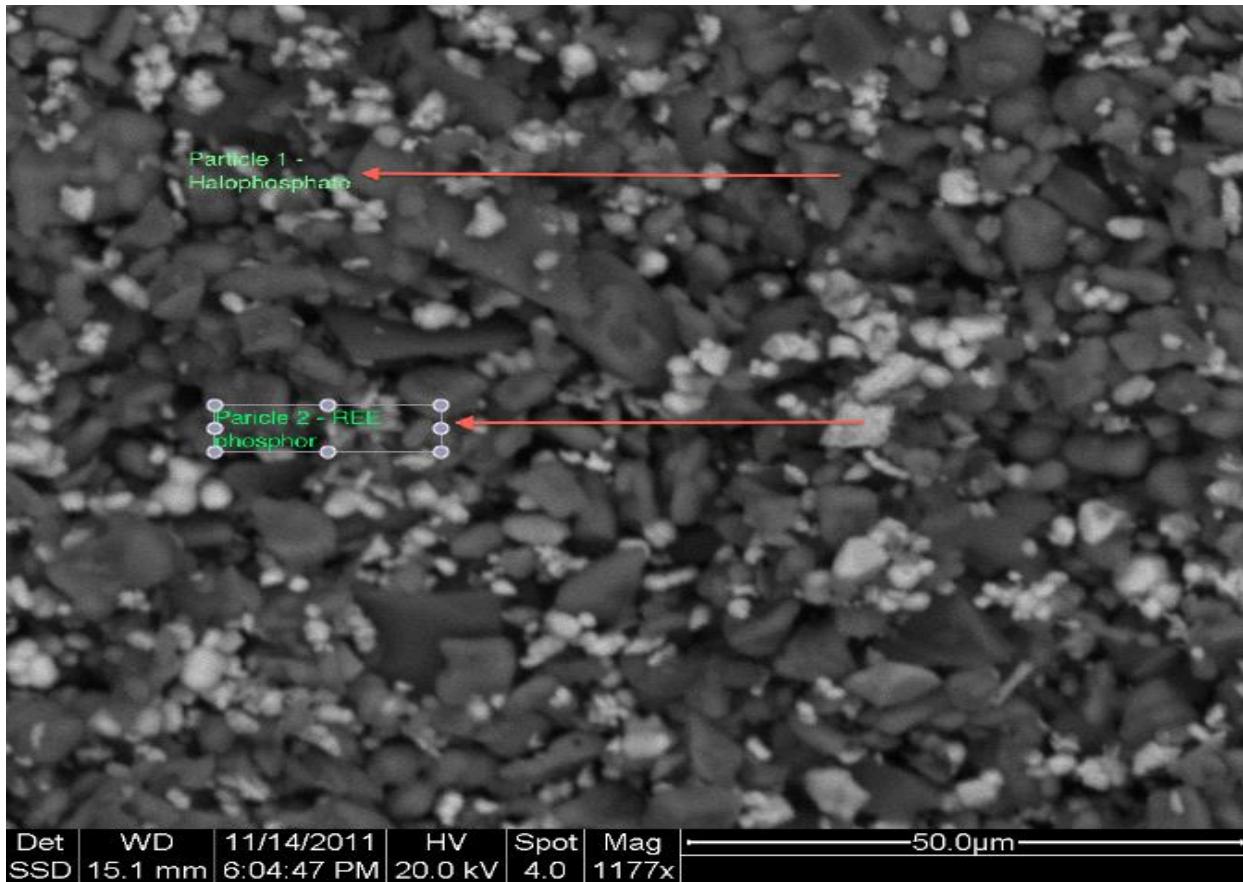
Figure 3.5: SEM of P_{10} fraction of REP showing dominance of two different particles.

CHAPTER 4

LEACHING

Acidic leaching has been a common method of extracting rare earths from naturally occurring minerals due to the tendency of the rare earths to be taken into solution easily at low pH and high eH. Thermodynamic modeling of rare earths on HSC has confirmed that acid leaching of rare earth minerals is not only possible but also relatively easy; therefore it was justified to experiment acid leaching on the phosphor dust.

The phosphor dust used in this experiment was obtained from Veolia Environmental Services. It is composed of waste second generation halophosphate lamps and third generation trichromatic phosphor lamps. Halophosphate lamps contains the white halophosphate phosphor, $(Sr,Ca)_{10}(PO_4)(Cl,F)_2:Sb^{3+},Mn^{2+}$ while the trichromatic phosphor lamps contain three main rare earth phosphors mixed in varying ratios to produce different colors of light. Trichromatic phosphors are transition metal compounds or rare earth compounds of various types. The commonly used trichromatic phosphors include: the red phosphor $Y_2O_3:Eu^{3+}$ (YOX), the green phosphors $LaPO_4:Ce^{3+},Tb^{3+}$ (LAP), $(Gd,Mg)B_5O_{12}:Ce^{3+},Tb^{3+}$ (CBT), $(Ce,Tb)MgAl_{11}O_{19}$ (CAT) and the blue phosphor $BaMgAl_{11}O_{17}:Eu^{2+}$ (BAM). The phosphor dust was generated by crushing the lamp tubes and removing mercury. The total rare earth elements (TREE) in the as-received powder were upgraded to 22.42% by sieving to below 44 μm. The P_{325} was then used for the leaching experiments. The chief rare earth elements in the phosphor powder are yttrium, europium, cerium, lanthanum and terbium.

4.1. Thermodynamic Modeling

The thermodynamic modeling was done with HSC Chemistry 5.11 and focused on terbium, europium and yttrium due to the increasing market price of these particular rare earth elements and thus better extraction and recoveries of these three would ensure maximum profitability.

Eh-pH diagrams for Ce-P-Cl-H_2O, La-P-Cl-H_2O, Tb-P-Cl-H_2O, Eu-Cl-H_2O and Y-Cl-H_2O systems at 100˚C had been previously generated and they show that it is thermodynamically feasible to get terbium, europium and yttrium into solution in an aqueous phase at pH values lower than 5 [69]. In order to test the feasibility of acid leaching of the phosphor dust at a lower temperature, Eh-pH diagrams were obtained for the most important rare earth systems at 70˚C as shown in Figure 4.1 - 4.5.

The redox state of metals and ligands that may complex them is the critical factor in the solubility of many metals. The Pourbaix diagrams for the chief rare earths in phosphor dusts below shows that the rare earths are soluble in HCl at pH less than 4 and Eu and Y dissolves significantly at higher or positive Eh values whereas cerium, terbium and lanthanum are mainly soluble at negative Eh values (highly reducing environment) thereby making these metals sparingly soluble in strong oxidizing agents like Cl. However, a similar phenomenon was observed in the RE-P-S-H_2O systems for these rare earths, thus by thermodynamics strong reducing agent such as sulfite in H_2SO_4 doesn't improve the dissolution or extraction of cerium, terbium and lanthanum from phosphors dust. The Pourbaix diagrams also show that at higher pH; yttrium, europium, cerium and lanthanum form RE-OH which is insoluble. This chemical property can be exploited in extracting the REE by first precipitating them as hydroxides and then solubilizing them in an acid media such as hydrochloric acid, nitric acid or sulfuric acid.
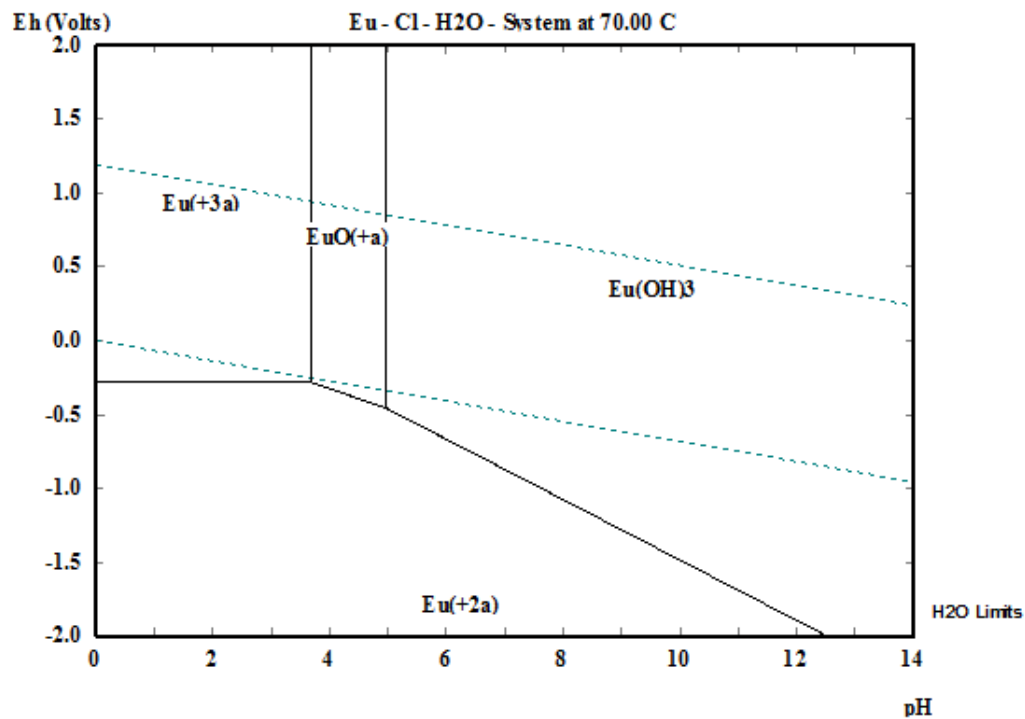
Figure 4.1: E_h-pH diagram for Eu-Cl-H_2O system at 70 ˚C.
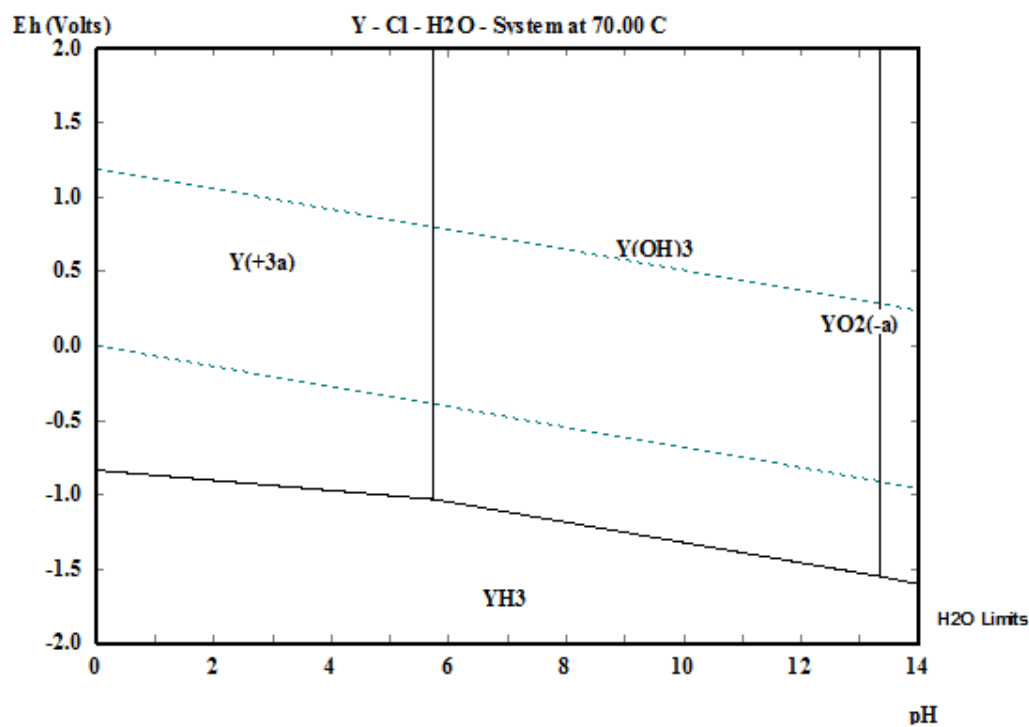
Figure 4.2: E_h-pH diagram for Y-Cl-H_2O system at 70˚C.
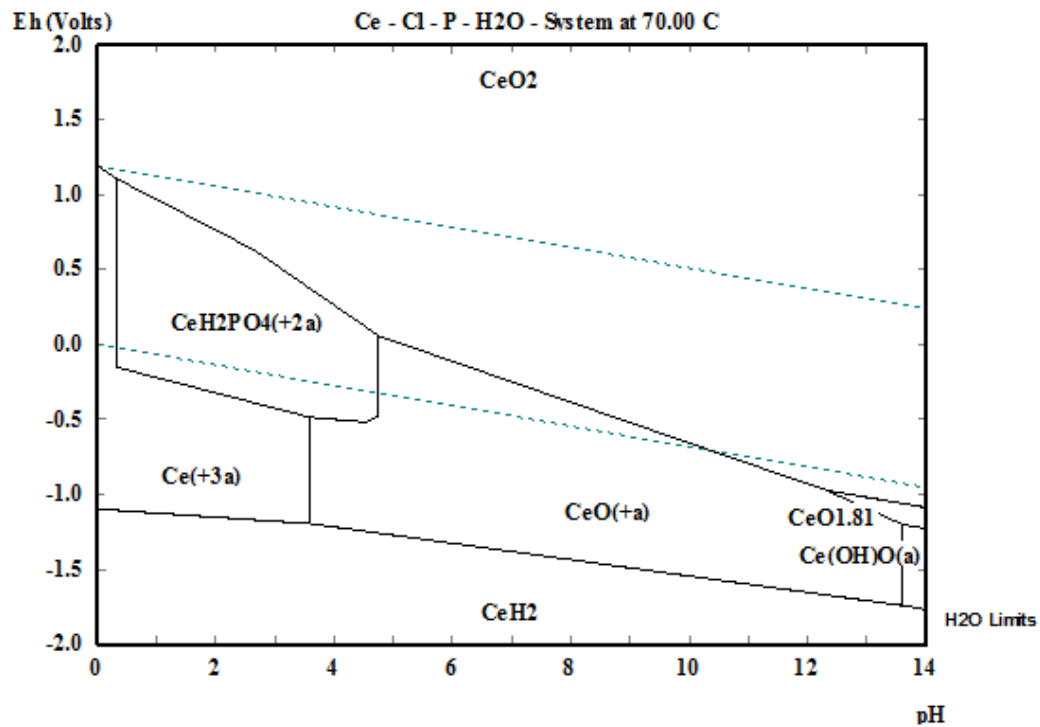
Figure 4.3: E_h-pH diagram for Ce-Cl-P-H$_2$O system at 70˚C.
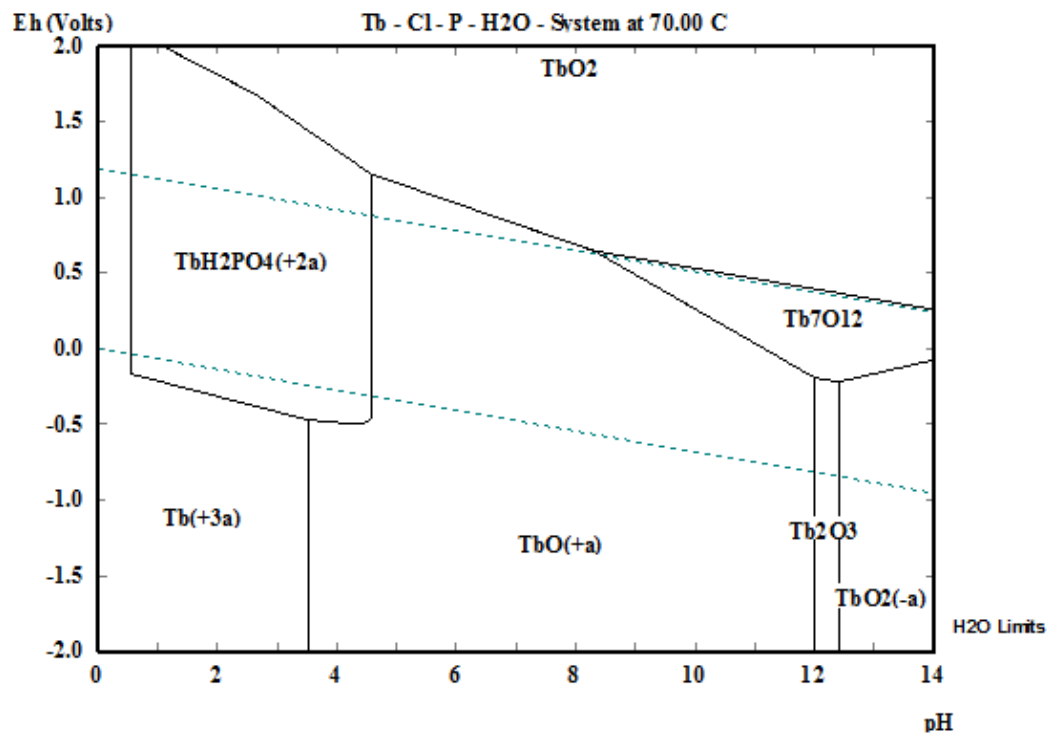
Figure 4.4: E_h-pH diagram for Tb-Cl-P-H$_2$O system at 70˚C.
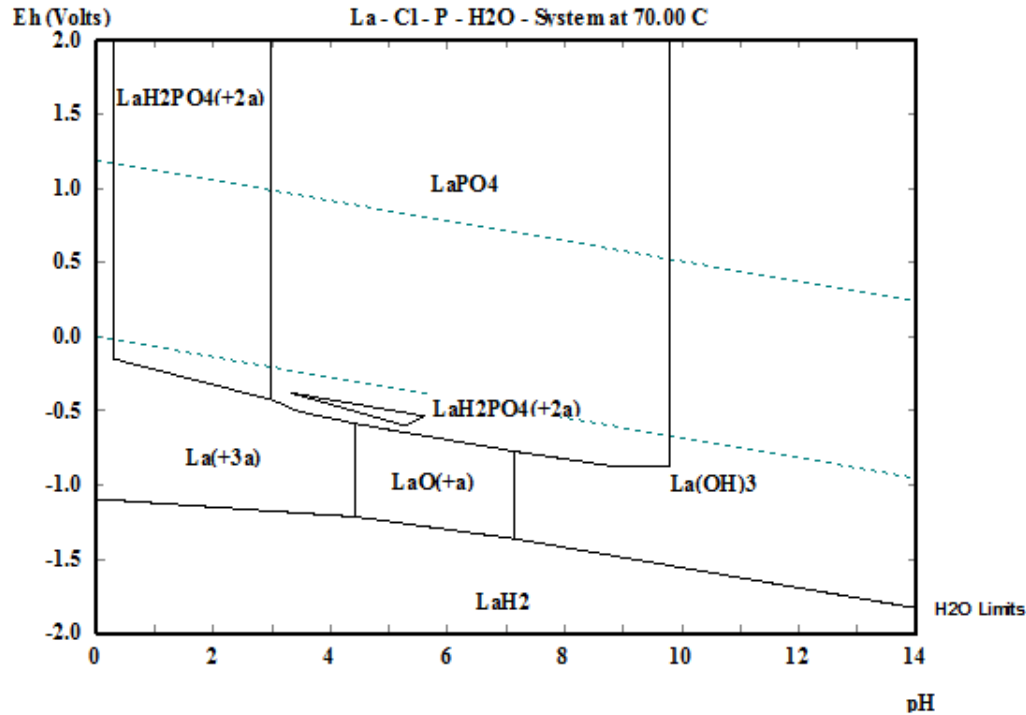
Figure 4.5: E_h-pH diagram for La-Cl-P-H_2O system at 70˚C.

4.2. Leaching Parameters

Based on literature review and thermodynamic modeling, it was understood that strong acids could be used to leach rare earths from the waste phosphors. Leaching with oxidizing acids has also been investigated by using hydrogen peroxide in combination with acid. However, results from batch leaching tests using this strong leachants yielded poor leaching efficiency especially for cerium, terbium and lanthanum since this elements exist as phosphates in the phosphor dust as shown in Table 4.1. Furthermore, this process isn't economical due to the high cost of using strong acids. Therefore a new approach utilizing a lower concentration of acid was recommended. Recent work carried out by Takahashi et al. (2003) studied hydrometallurgical separation and recovery of rare earths from phosphors in the fluorescent lamp wastes using sulfuric acid leaching at different conditions. The optimized leaching condition after those series of studies are: sulfuric acid concentration of 1.5 M, temperature of 70˚C, leaching time of 1 hour,

and S/L of 30 g/L. A feasibility test was performed using those optimized conditions as reference in order to identify the best conditions for extracting the REEs from the phosphor dust obtained. The following parameters were investigated: leaching reagent, acid concentration, temperature, leaching time, agitation and pulp concentration. Table 4.2 below lists the distribution of the main elements in the powder used for the optimization process.

Table 4.1: Batch leaching test under strong leaching conditions from feasibility study.

Strong Leaching Conditions	% Extraction				
	Ce	Tb	La	Eu	Y
2.5 M HNO_3 60 g/L 90 ˚C 1 hr 200 rpm	0.44	0.72	1.52	53.55	56.22
4 M H_2SO_4 30 g/L 70 ˚C 4 hr 600 rpm	BDL*	0.71	0.25	56.00	83.75
4 M HCl 50 g/L 90 ˚C 4 hr 600 rpm	2.15	22.45	35.24	95.56	100
4 M HCl + 4.4 g/L H_2O_2 30 g/L 60 ˚C 4 hr 600 rpm	1.53	2.05	3.74	74.37	77.01
4 M HCl + 4.4 g/L H_2O_2 100 g/L 60 ˚C 4 hr 600 rpm	0.17	0.90	3.43	76.84	71.72
6 M HCl 30 g/L 70 ˚C 4 hr 200 rpm	3.80	5.80	6.17	92.93	94.08

BDL* - Below Detection Limit

Table 4.2: Major elemental composition of the powder used for leaching experiments.

Feed Composition	
	% wt
Ce	2.86
Eu	0.78
La	2.65
Nd	0.76
Pr	0.86
Sm	0.96
Tb	1.21
Y	10.81
Al	2.93
Ca	19.01
Fe	0.29
P	10.24
Si	4.63

4.2.1. Effect of Leaching Reagent

Different acidic and basic reagents were tested at the reference leaching conditions to determine which medium gives the highest leaching efficiency. Different isotonic leaching reagents (1.5 M) were used: hydrochloric acid, sulfuric acid, nitric acid and sodium hydroxide. All the experiments were carried out with the same leaching conditions: temperature of 70˚C, leaching time of 1 hour, and S/L ratio of 30 g/L.

Figure 4.6 shows that basic leaching by NaOH results in very low rare earth extraction ($\leq$ 1%) and thus not suitable to recover rare earth elements from phosphor dust. H_2SO_4 and HNO_3 leaching systems gave similar results in Ce, Tb, La, Eu and Y extraction but the former showed the advantage of the significant reduction of Ca extraction into the leach liquor with subsequent advantage during downstream purification process (Table 4.3) whereas the latter was rejected because red toxic gases of NO and NO_2 were generated. HCl gave the highest Eu and Y extraction although there was also higher dissolution of impurities as shown in Table 4.3. Ce, Tb and La all showed poor dissolution in both basic and acidic leaching systems. HCl was therefore established as the leachate of choice because of the highest leaching efficiency and also it is already being used extensively in most rare earth extraction processes.

Table 4.3: The level of extraction of impurities from powder into the acid reagent.

Elements	% Extraction		
	1.5 M HCl, 70˚C, 30 g/L, 1 hr, 200 rpm	1.5 M H_2SO_4, 70˚C, 30 g/L, 1 hr, 200 rpm	1.5 M H_2SO_4, 70˚C, 30 g/L , 3 hr, 200 rpm
Al	38.71	33.66	41.91
Ca	98.24	11.43	12.92
Fe	97.61	93.51	92.82
Mg	20.46	21.34	20.46
Na	17.12	16.49	17.79
P	94.29	92.68	91.85
Si	10.23	10.31	10.23
Zn	81.29	76.98	76.26

Figure 4.6: Bar chart showing the % extraction of the important REE from the phosphor dust with different leaching reagent. Other leaching parameters: Time = 1 hr,
Temp. = 70 ˚C, S/L = 30 g/L, Agitation = 200 rpm.

4.2.2. Effect of Acid Concentration

The reference conditions set up for batch leaching tests were a temperature of 70˚C, solid to liquid ratio of 30 g/L, leaching time of 1 hour and agitation of 200 rpm. Figure 4.7 below shows the variation in extraction of total rare earths from the powder into solution under different concentration of acid. With increasing acid concentration the extraction increases significantly initially and then plateaus beyond 2 M.

REE extraction increases with increasing acid concentration. Eu and Y extraction reaches substantially high values with acid concentrations of 1.5 M whereas Ce, Tb and La extraction continues to increase throughout although they remain significantly low. Figure 4.8 below shows the extraction of the individual rare earth elements as a function of acid concentration.
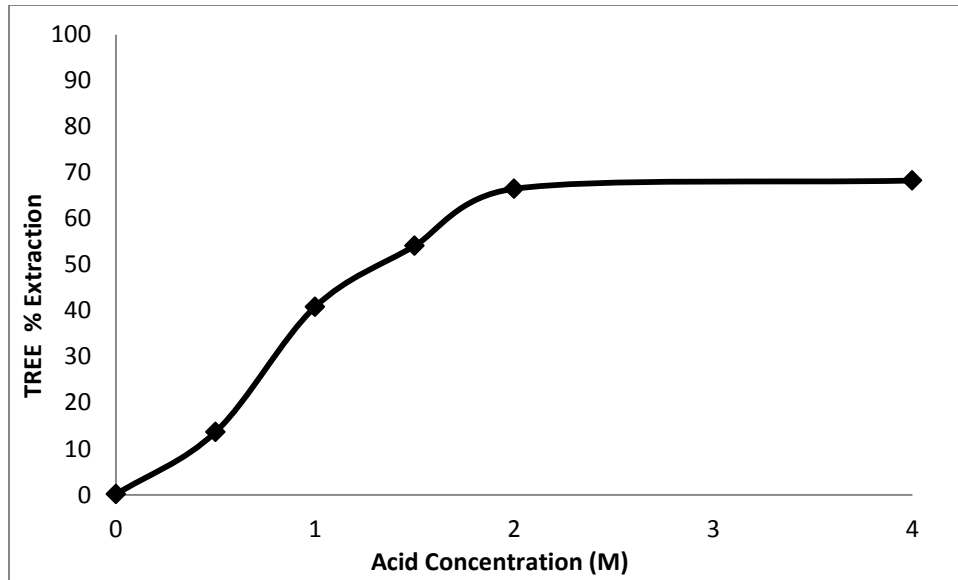
Figure 4.7: Graph showing the % extraction of TREE with different concentrations of hydrochloric acid. Other leaching parameters: Time = 1 hr, Temp. = 70 ˚C, S/L = 30 g/L, Agitation = 200 rpm.

Figure 4.8: Bar chart showing the % extraction of the important REE from the phosphor dust with varying HCl concentration. Other leaching parameters: Time = 1 hr, Temp. = 70 ˚C, S/L = 30 g/L, Agitation = 200 rpm.

4.2.3. Effect of Temperature

The temperature for the experiment was varied from 25˚C to 80˚C while the other leaching parameters were held constant at the reference conditions. Figure 4.9 shows that the total rare earth extraction increases by 40% on increasing the temperature from 25˚C to 50˚C and increases till 70˚C and then decrease by about 1% at 80˚C. Thus leaching at 90˚C wasn't considered. The highest extraction of Eu and Y occurred at 70˚C but it wasn't significantly greater than at other temperatures except at 25˚C. Ce extraction was below detection level. Fluctuation in the level of Tb and La extraction was observed. Figure 4.10 shows the individual rare earth extractions at varying temperature.
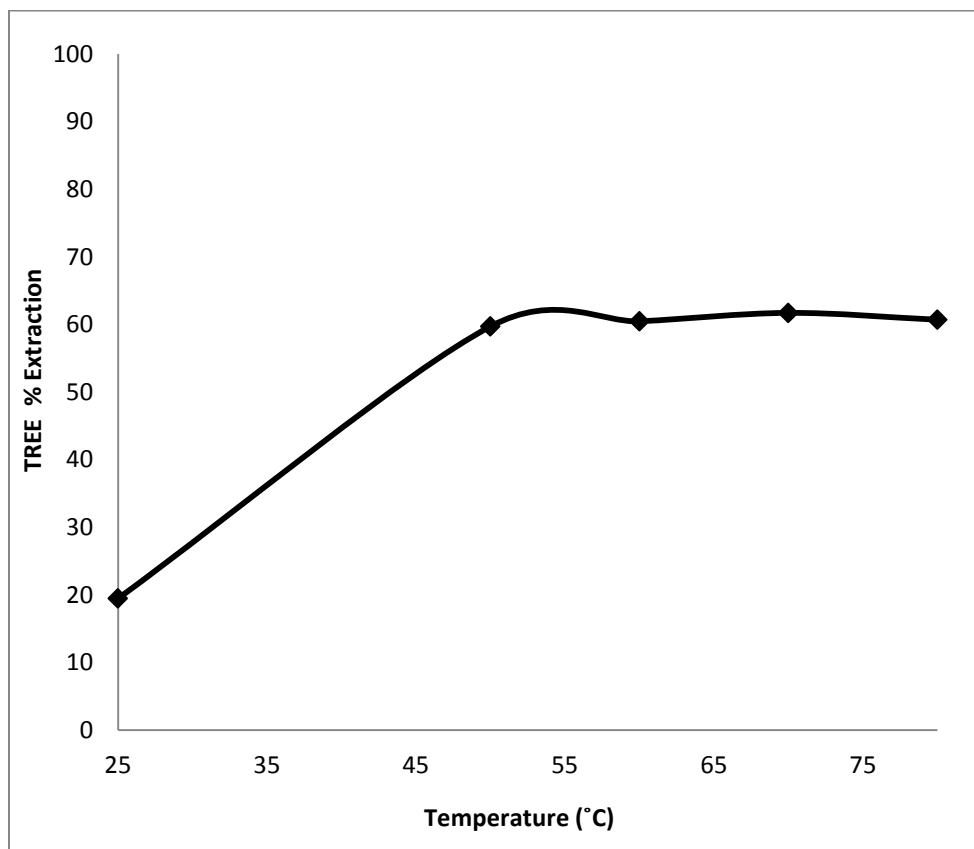
Figure 4.9: Graph showing the % extraction of TREE at different temperatures. Other leaching parameters: Time = 1 hr, Acid Conc. = 1.5 M, S/L = 30 g/L, Agitation = 200 rpm.
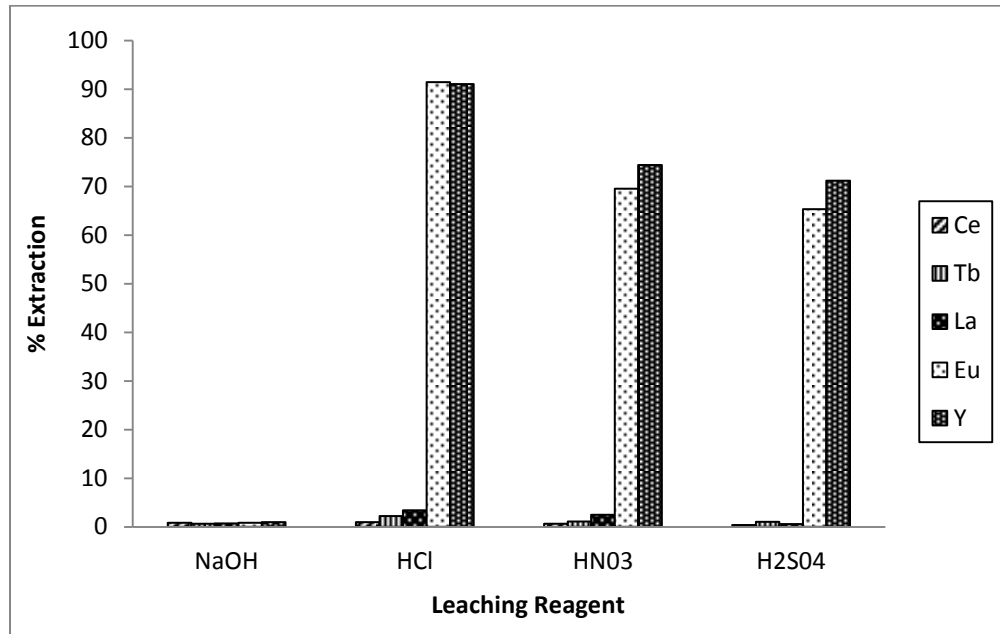
Figure 4.10: Bar chart showing the % extraction of the important REE from the phosphor dust at different temperatures. Other leaching parameters: Time = 1 hr, Acid Conc. = 1.5 M, S/L = 30 g/L, Agitation = 200 rpm. Temp. = 70 ˚C, S/L = 30 g/L, Agitation = 200 rpm.

4.2.4. Effect of Leaching Time

In order to optimize the leaching efficiency for maximum total rare earth extractions, the leaching time was varied while the other leaching parameters were held constant at the reference conditions. It can be seen from Figure 4.11 and 2.12 that total rare earths increases steadily from 0.5 hr to 3 hr but drops by about 7% at 4 hr. Maximum recoveries of all the chief REEs was obtained at 3 hr which represents the optimal leaching time but the level of extraction was it was significantly greater than those obtained at 1 hr.
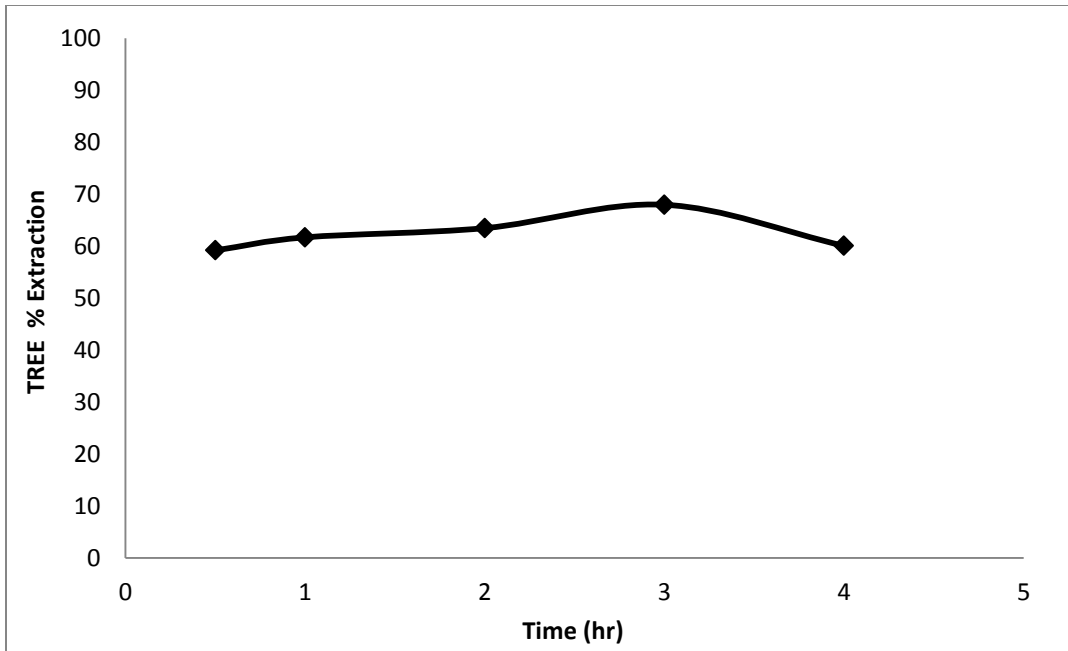
Figure 4.11: Graph showing the % extraction of TREE at different temperatures. Other leaching parameters: Acid Conc. = 1.5 M, Temp. = 70 ˚C, S/L = 30 g/L, Agitation = 200 rpm.

Figure 4.12: Bar chart showing the % extraction of the important REE from the phosphor dust at different temperatures. Other leaching parameters: Acid Conc. = 1.5 M, Temp. = 70 ˚C, S/L = 30 g/L, Agitation = 200 rpm.

4.2.5. Effect of Solid-Liquid Ratio (S/L)

The solid to liquid ratio is critical for the leachability of metals because it controls acid consumption and the interaction between the leachant and the feed particles. The solid to liquid ratio was varied between 30 g/L to 120 g/L and the other leaching parameters held at the reference conditions.

It is evident from Figure 4.13 that the S/L ratio tested resulted in low total rare earth extraction although the extraction of Eu and Y is markedly high as shown in Figure 4.14. Beyond 30 g/L the extraction drops significantly from 54.10% to as low as 6.89%.

Figure 4.13: Graph showing the % extraction of TREE at different S/L ratio. Other leaching parameters: Time = 1 hr, Acid Conc. = 1.5 M, Temp. = 70˚C, Agitation = 200 rpm.
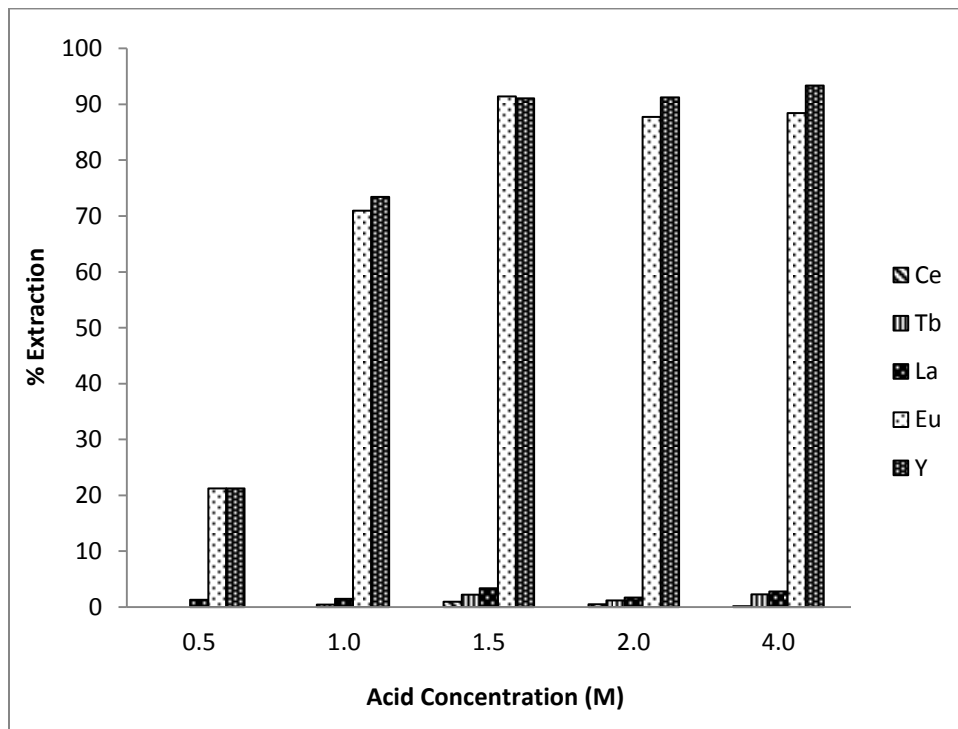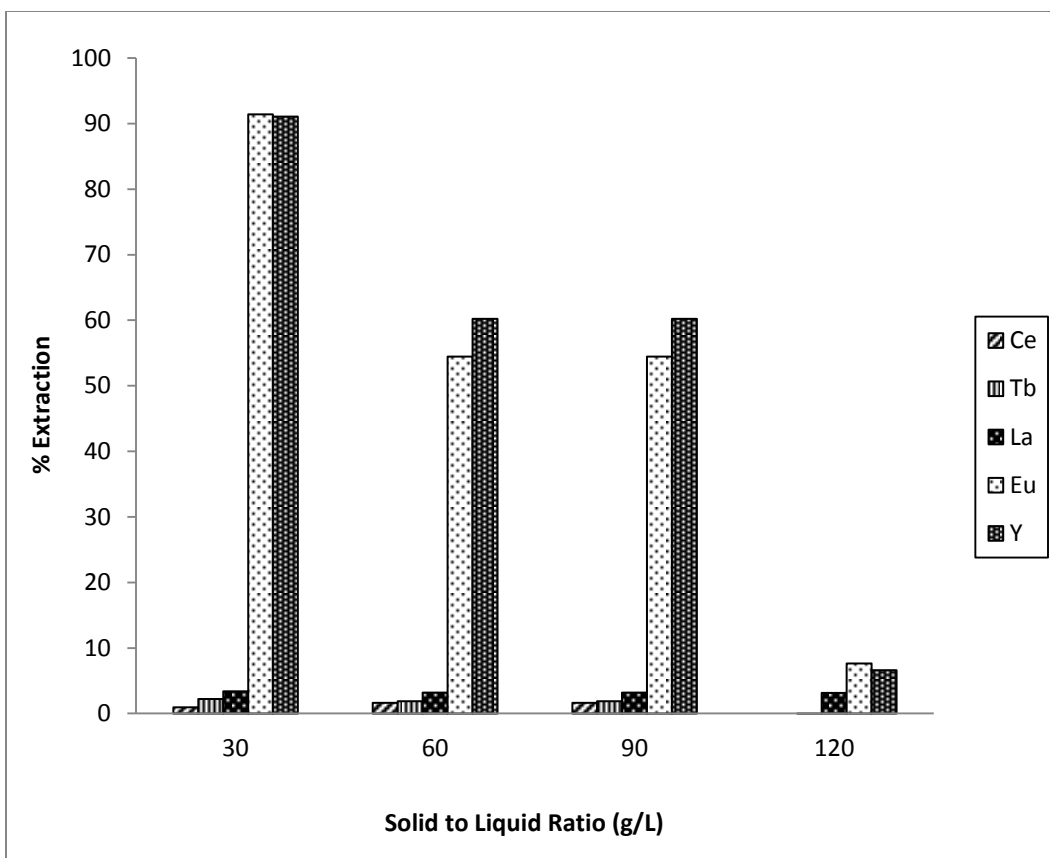
Figure 4.14: Bar chart showing the % extraction of the important REE from the phosphor dust at different S/L ratio. Other leaching parameters: Time = 1 hr, Acid Conc. = 1.5 M, Temp. = 70 °C, Agitation = 200 rpm.

4.2.6. Effect of Agitation Speed

Optimum agitation aids in increasing the rate of a heterogeneous reaction. In order to optimize the agitation, the system was agitated to speeds varying from 200 rpm to 600 rpm while the other leaching parameters were held constant at the reference conditions. The extractions were highest at 200 rpm and upon further increasing the agitation speed to 600 rpm, the total rare earth extraction decreased slightly and steadily as shown in Figure 5.14. It can be observed from Figure 5.15 that leaching at higher speed doesn't improve the individual rare earths significantly. Eu and Y extractions reduces by about 17% and 10% respectively whereas a fluctuation is observed in Ce, Tb and La extraction although there is a slight increase.
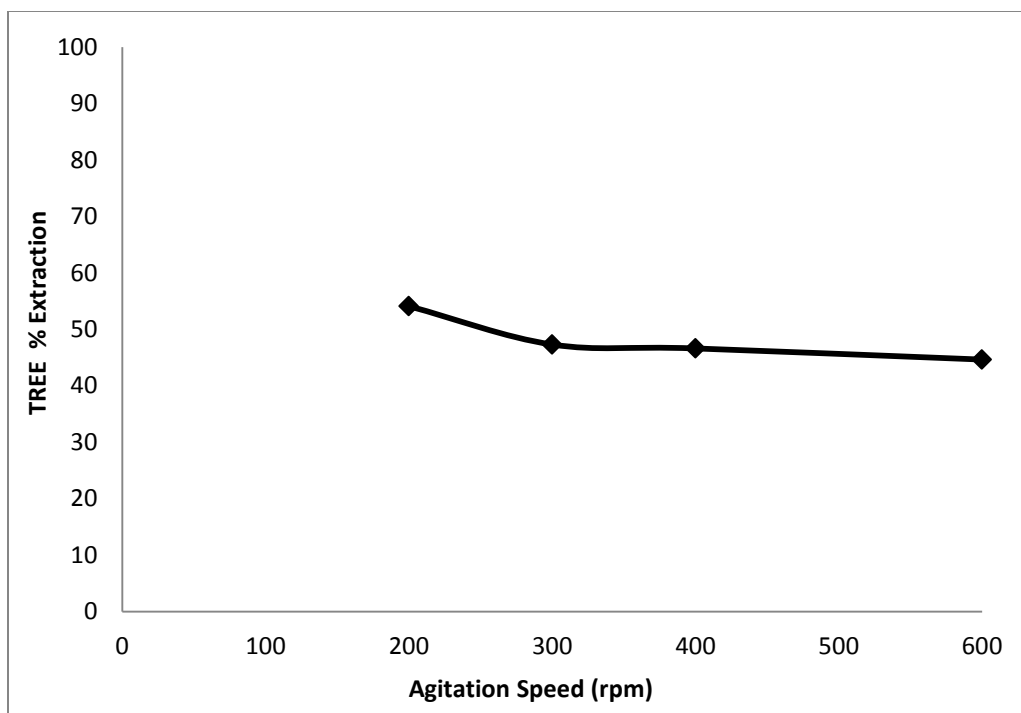
Figure 4.15: Graph showing the % extraction of TREE at different agitation speed. Other leaching parameters: Time = 1 hr, Acid Concentration = 1.5 M, Temp. = 70˚C, S/L = 30 g/L.
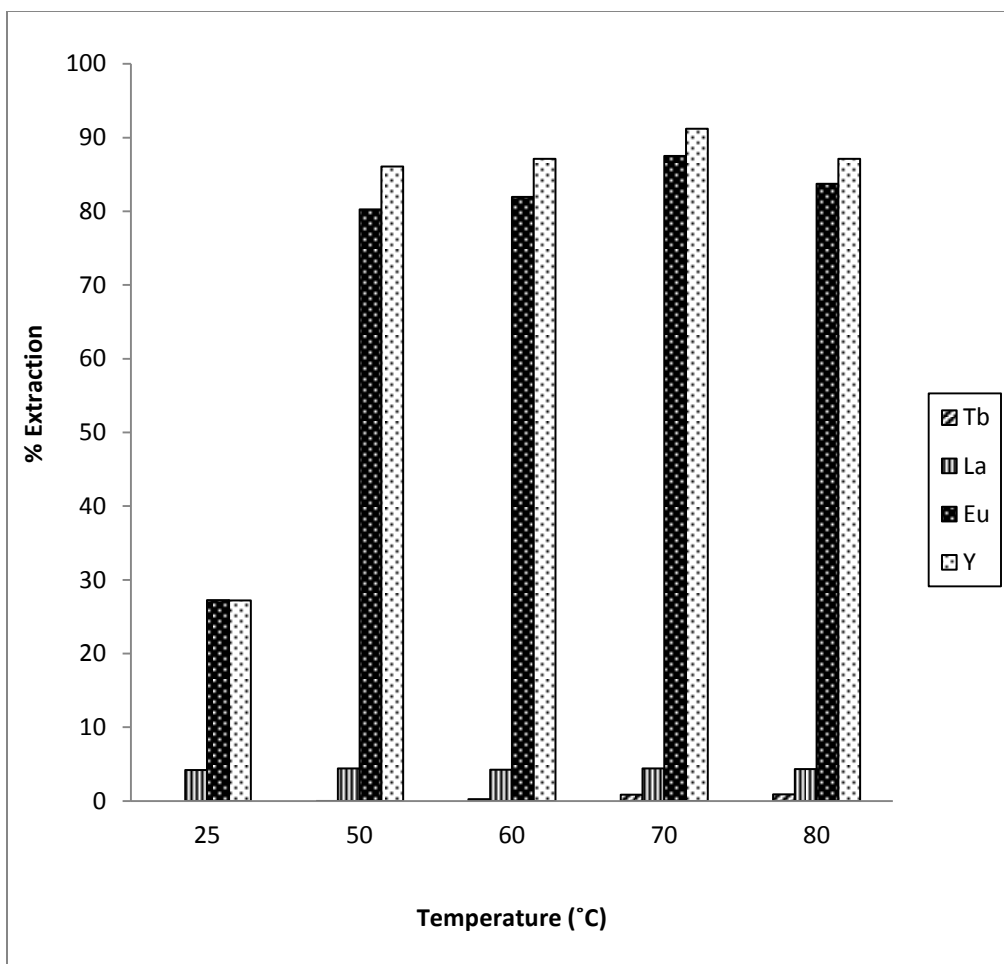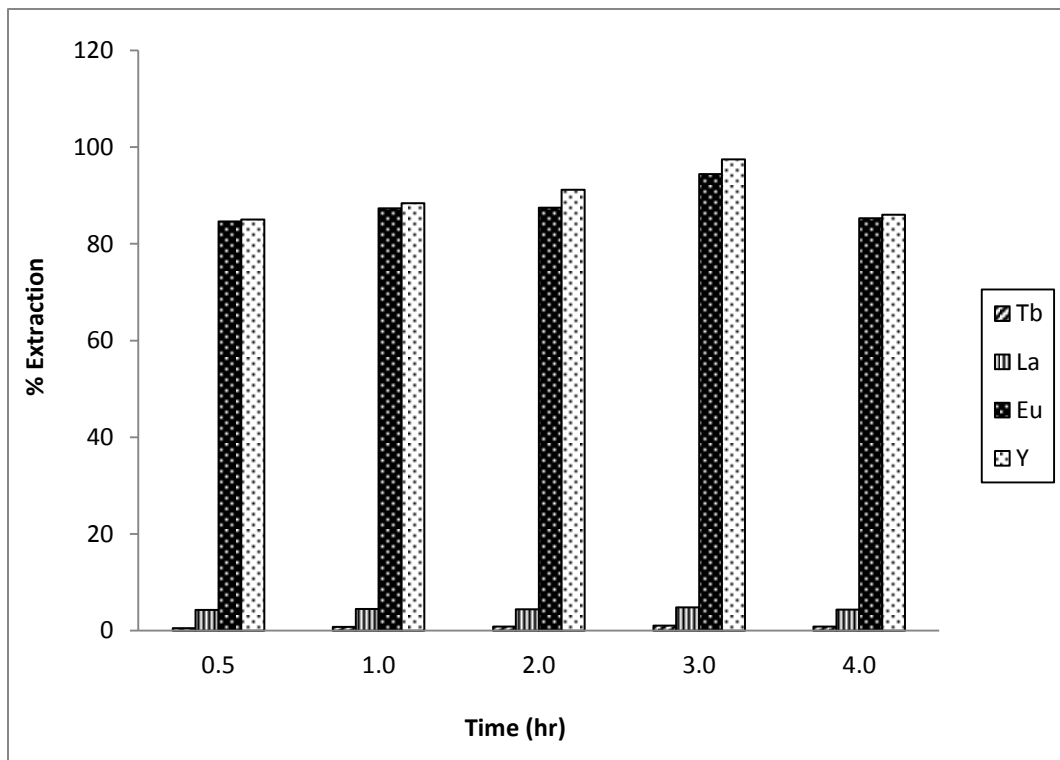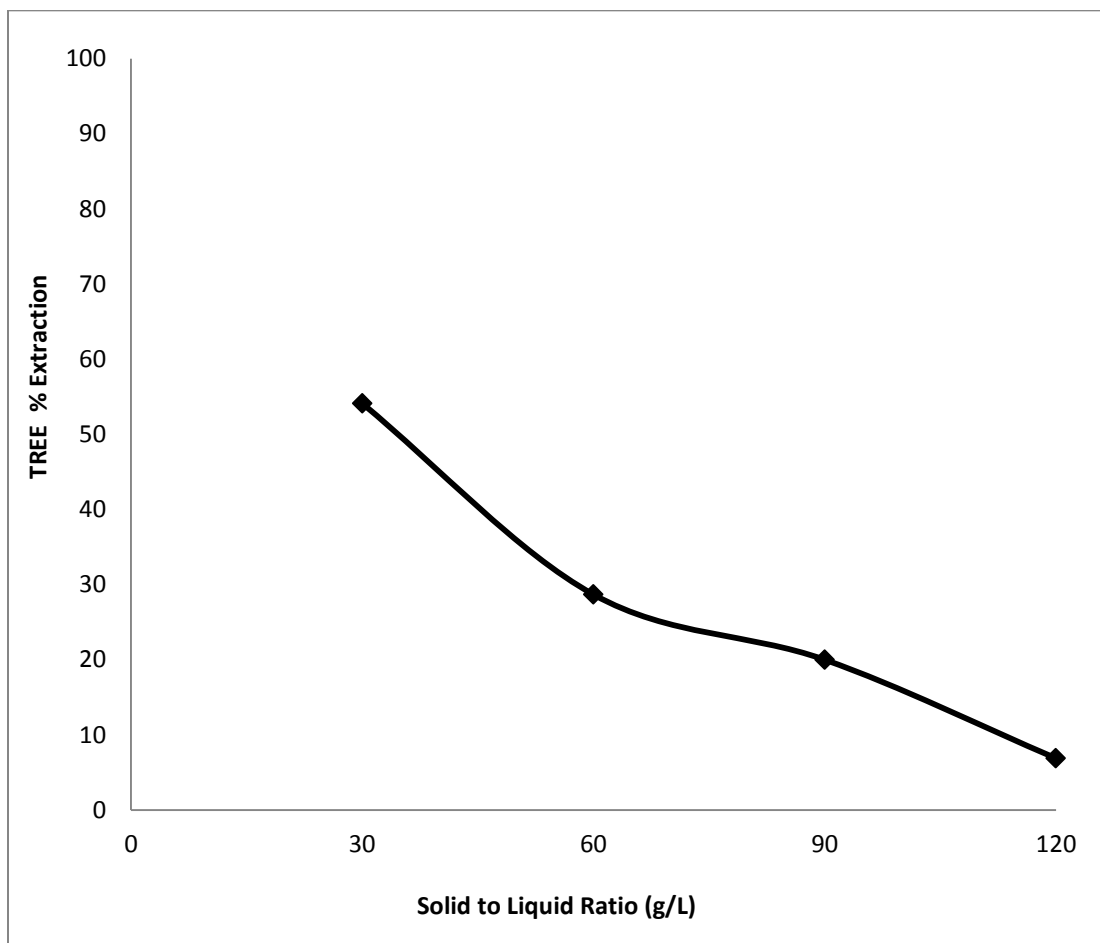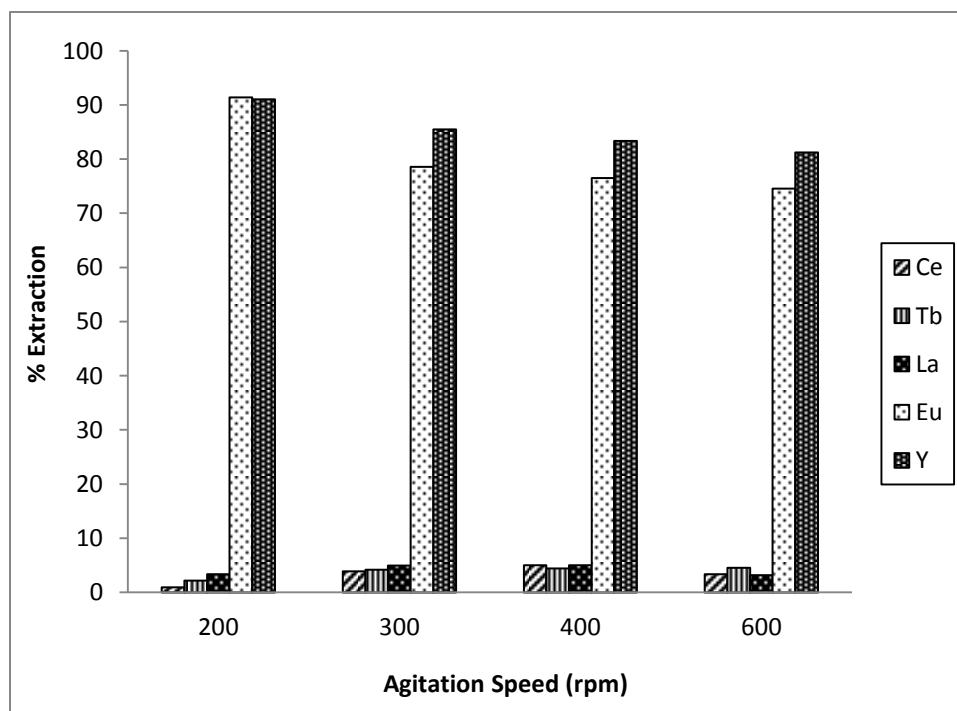

Figure 4.16: Bar chart showing the % extraction of the important REE from the phosphor dust at different agitation speed. Other leaching parameters: Time = 1 hr, Acid Conc. = 1.5 M, Temp. = 70 ˚C, S/L = 30 g/L.

4.2.7. Optimized Leaching Conditions

Despite the fact that rare earths are reactive metals, Ce, Tb and La were not taken into solution by both weak and strong acids. This is partly because of the acid preferentially attacking other impurities in the powder and the nature of the rare earth compounds. The feasibility tests for process optimization shows that the best extractions from the phosphor dust were observed at the following conditions: 1.5 M HCl, 30 g/L, 70°C, 1 hr and 200 rpm. Under these conditions there is high extraction of Eu and Y ($\approx$ 91%) but there is poor dissolution of Ce, Tb and La because these elements exist as phosphates while Eu and Y are oxides in the powder. There is also co-dissolution of other elements such as Al, Ca, Na, P, Mg, Fe Si and Zn during leaching and they constitute impurities in the leachate which have to be removed in downstream purification processes. These optimized conditions were also chosen because it is cost-effective since leaching at higher acid concentration (2 - 4 M) didn't result in a significant improvement on the extraction of the rare earths, especially Ce, Tb and La, in comparison to leaching at 1.5 M.

In order to make the process cost-effective and economically attractive it is essential to increase extraction of all five chief rare earths in the powder. This feasibility test and previous studies show that one-step or direct acid leaching using mild or strong acid reagents isn't efficient for the extraction of all chief rare earths and therefore an efficient process such as multistage leaching has to be investigated and developed for optimum recovery.

4.3. Multistage Leaching

The varying level of extraction of europium and yttrium from lanthanum, terbium and cerium is quite significant implying varying level of solubility of the phosphors containing each of these elements. The extraction of europium is slightly lower than yttrium under the various

conditions investigated due to low solubility of BAM phosphor which also contains 1 - 5% europium.

The higher solubility of the Eu and Y containing phosphor can hence be exploited to increase overall recovery. The process can effectively be broken down into a multistage leach process with the first leaching step being with a dilute acid or base to collect the Eu and Y fraction. The residue is then sent to a second leaching step under a strong oxidizing environment with strong acid. During the first leaching step with NaOH, there is a conversion of rare earths oxides and phosphates in the powder to an insoluble hydroxide residue of rare earths which are then solubilize by the acid leach. Thus a strong second leaching step could significantly increase the extraction of total rare earths as well and increased extraction of cerium, lanthanum and terbium while ensuring better acid consumption.

Table 4.4: Second stage acid leach results from multistage leaching test.

Two stage Leach Conditions	% Extraction				
	Ce	Tb	La	Eu	Y
1.5 M NaOH 30 g/L 70 ˚C 1 hr 200 rpm 6 M H₂SO₄ 30 g/L 90 ˚C 1 hr 600 rpm*	0.53	1.65	1.22	76.36	94.13
1.5 M NaOH 30 g/L 70 ˚C 1 hr 200 rpm 4 M HCl + 4.4 g/L H₂O₂ 30 g/L 60 ˚C 1 hr 600 rpm*	35.55	35.03	59.90	92.44	99.46
1.5 M NaOH 30 g/L 70 ˚C 1 hr 200 rpm 6 M HCl 30 g/L 90 ˚C 1 hr 200 rpm*	40.07	40.18	65.80	84.76	95.69
1.5 M HCl 30 g/L 70 ˚C 1 hr 200 rpm 6 M HCl 30 g/L 90 ˚C 1 hr 200 rpm*	69.43	73.61	84.94	1.76	0.67

* Second stage strong acid leach

Using dilute NaOH in the first leaching step extracts less than 1% of Eu and Y but all subsequent acid leach tested in Table 4.4 above removed significant amount of Eu and Y especially when hydrogen peroxide was added to increase the oxidizing power of the acid.

However, the extraction Ce, Tb and La in the tests were still poor except when dilute HCl was used in first leaching step. This is because the dilute HCl removes over 90% of Eu and Y producing a Ce, Tb and La concentrate for the second leaching step which then enables better extraction of these three rare earths. There is an increase in total rare earth extraction under this multistage leaching process with dilute and concentrated acid primarily due to the improvement of La extraction. However, the extraction of Tb, one of the rare earths with high market price, is still not satisfactory for maximum profitability. Therefore, a different process has to be developed to effectively decompose the rare earth phosphate, $LaPO_4:Ce^{3+}$, Tb^{3+} (LAP), in the phosphor dust to make them more amenable to leaching and there by attain optimum Tb extraction. Tb is relatively easier to extract from the other green phosphors $(Gd,Mg)B_5O_{12}:Ce^{3+},Tb^{3+}$ (CBT), $(Ce,Tb)MgAl_{11}O_{19}$ (CAT) because they are oxides.

CHAPTER 5

THERMAL TREATMENT AND NEW PROCESS DEVELOPMENT

In the industrial processing of rare earth minerals, high temperature treatments such as calcining and roasting is employed to decompose the minerals to allow easy recovery of the rare earth values. Merritt (1990) has suggested high temperature processes for breaking down the phosphate matrix in monazite by sintering with sodium carbonate at 900°C and with sodium carbonate and flux at 800°C - 825°C. The main advantage of the high temperature process is that thorium does not contaminate the rare earth concentrate as much but these processes give lesser recovery rates when compared to the alkaline route. Merritt (1990) has also suggested a process involving high temperature reaction (980°C - 1190°C) of monazite with calcium chloride and calcium carbonate to decompose the monazite and produce rare earth oxysulfides, oxychlorides, a thorium rich oxide solid solution, and a calcium chlorophosphate (chloropatite). The rare earth elements are then removed by leaching with 3% HCl. Although the process gives poor recovery of phosphate, it allows for a short time to decompose all the monazite and grinding of the ore to ~50 µm is not necessary. Furthermore the thorium oxide residue from the dilute acid leach is readily filtered and disposed by burial. When sodium carbonate is used as reactant for attacking the monazite at 900°C in an environment that is both reducing and sulfidizing, the problem with phosphate recovery is solved since γ-trisodium phosphate and a mixed sodium rare earth element phosphate is formed and most of the phosphate can then be recovered by leaching with water at room temperature.

The decomposition of bastnasite by heat treatment has also been extensively studied. In the Molycorp process (World Mining 1966), the crude bastnasite ore (Mountain Pass) is crushed and ground and subjected to multistage floatation to obtain a 60% REO concentrate which is then roasted in air at 620°C to remove carbon dioxide and decompose the carbonate in the lattice, thereby reducing acid consumption. Roasting also oxidizes cerium (Ce^{3+}) to the tetravalent state (CeO_2), which does not readily dissolve in the acidic lixiviant, instead reporting to the leach residue which is sold directly, or treated for cerium recovery. After roasting, the calcine is treated with 30% HCl to dissolve the non-cerium rare earths yielding a marketable cerium concentrate containing 65 - 70% REO and 55% - 50% CeO_2. In another process, the floatation concentrate is first upgraded to about 70% REO by leaching with HCl to remove impurities such as calcium and strontium carbonates. Subsequent roasting can further increase the REO content to 85 - 90% by liberating carbon dioxide from the carbonate portion of the mineral.

Following the thermal treatment approach of the rare earth minerals, the phosphor dust was calcined at various temperatures to investigate the decomposition of the rare earth phosphate in the powder and thereby improve the leachability of terbium. The main rare earth phosphors commonly used in trichromatic fluorescent lamps include: the red phosphor Y_2O_3:Eu^{3+} (YOX), the green phosphors $LaPO_4$:Ce^{3+},Tb^{3+} (LAP), (Gd,Mg)B_5O_{12}:Ce^{3+},Tb^{3+} (CBT), (Ce,Tb)$MgAl_{11}O_{19}$ (CAT) and the blue phosphor $BaMgAl_{11}O_{17}$:Eu^{2+} (BAM). YOX and LAP are almost 100% rare earth compounds and BAM contains 1 - 5% europium oxide. The LAP phosphor is a rare earth phosphate and contains lanthanum, cerium and terbium and its thermal decomposition and amenability to acid leaching is critical for improving the extraction of terbium.

5.1. Thermal Decomposition of LAP Phosphor at Low Temperature

The appropriate ranges of thermal treatment process to be studied experimentally were examined using HSC Chemistry 5.11 in order to determine the chemical compounds formed during the process as well as the temperatures they form. Lanthanum phosphate is present in bulk amounts in LAP phosphor so it was chosen for the thermodynamic modeling. Equilibrium composition diagram of the thermal decomposition reaction of lanthanum phosphate with sodium carbonate was generated to determine the feasibility of this calcination process and also the properties of the primary and by-products formed as shown in Figure 5.1 below.
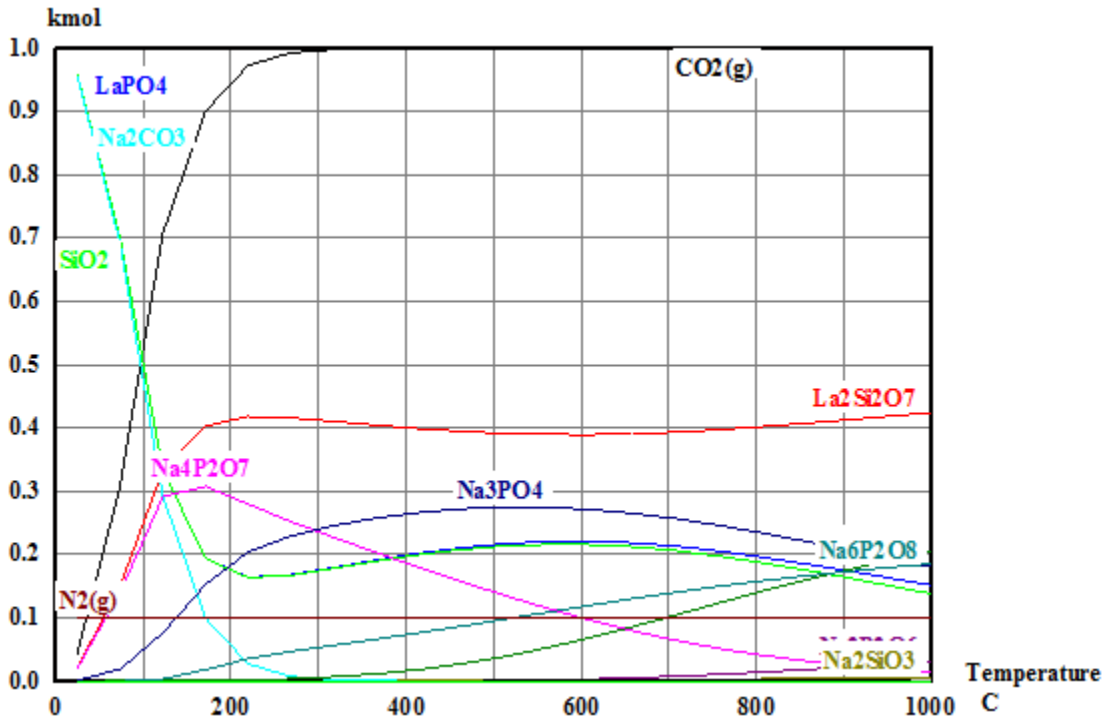
Figure 5.1: Thermal decomposition diagram of $LaPO_4$ during calcination with Na_2CO_3. Input: 1 Kmole $LaPO_4$ and Kmole Na_2CO_3.

From Figure 5.1, it can be seen that it possible to break down $LaPO_4$ at 200°C during calcination with Na_2CO_3. Over 80% of $LaPO_4$ decompose to LaO_2 (gas) and La_2O_3, which is

soluble in acids and slightly soluble in water. Significant amount of carbon dioxide is also generated and have to be scrubbed with NaOH which will extra cost to the process.

After the thermodynamic analysis, the feasibility of the calcination process was further studied experimentally by heating the phosphor dust with Na_2CO_3 at 400˚C in a Muffle furnace at different calcination times to convert the rare earth phosphates in the powder to rare earth oxides (REOs). Although the thermodynamic model shows the reaction is favorable at 200˚C, the calcination process was carried out at 400˚C to compensate for energy absorbed by the other constituents in the powder. The calcine was then leached with different acids to solubilize the rare earth values. The results for this calcine-leach process are shown in Table 5.1 below.

Table 5.1: Results of calcine-leach process on the powder with sodium carbonate.

Calcine-Leach Process Conditions	% Extraction		
		1 hr	2 hr
A. 1 g Phosphor Dust + 3g Na_2CO_3 B. 6 M HCl, 10 g/L, 90 °C, 1 hr, 200 rpm	Ce	28.99	29.55
	Tb	30.18	30.22
	La	33.88	34.68
	Eu	87.89	93.14
	Y	89.38	95.95
A. 1 g Phosphor Dust + 3g Na_2CO_3 B. 6 M HNO_3, 10 g/L, 90 °C, 1 hr, 200 rpm	Ce		35.01
	Tb		34.78
	La		39.36
	Eu		91.91
	Y		94.28

A - Calcination conditions
B - Leaching conditions

Although the thermodynamics of breaking the phosphate matrix in the LAP phosphor by calcining with Na_2CO_3 is favorable, the actual experiment yielded poor recoveries of Ce, Tb and La. This may be because the chemistry of the reaction between $LaPO_4$ and Na_2CO_3 changed in the presence of the other compounds in the powder. Increasing the calcination time to 2 hours

had minimal impact on the rare earth phosphates conversion rate although the level of extraction of Eu and Y increased to high values. Furthermore leaching the calcine with HNO_3 was slightly better than using HCl.

5.2. Thermal Decomposition of LAP Phosphor at High Temperature

Equilibrium composition diagrams of the decomposition reaction of lanthanum phosphate in oxidizing (air), reducing (with CO), sulfidizing (with SO_2) and chloridizing (Cl_2) atmospheres at temperatures ranging between 500°C and 2000°C were generated (Figure 5.1 - 5.5). This was to model the thermal decomposition of the LAP phosphor at high temperatures before studying the calcine-leach process at these temperatures experimentally.
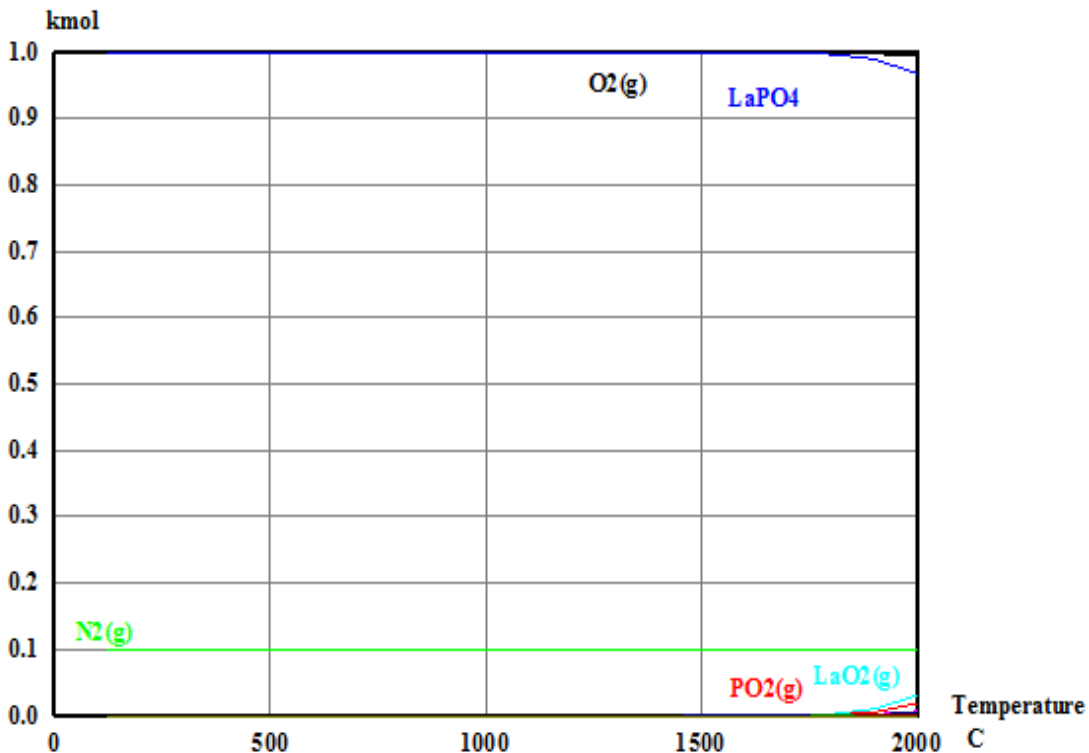
Figure 5.2: Thermal decomposition diagram of $LaPO_4$ in air. Input: 1 Kmole $LaPO_4$ and Kmole O_2.
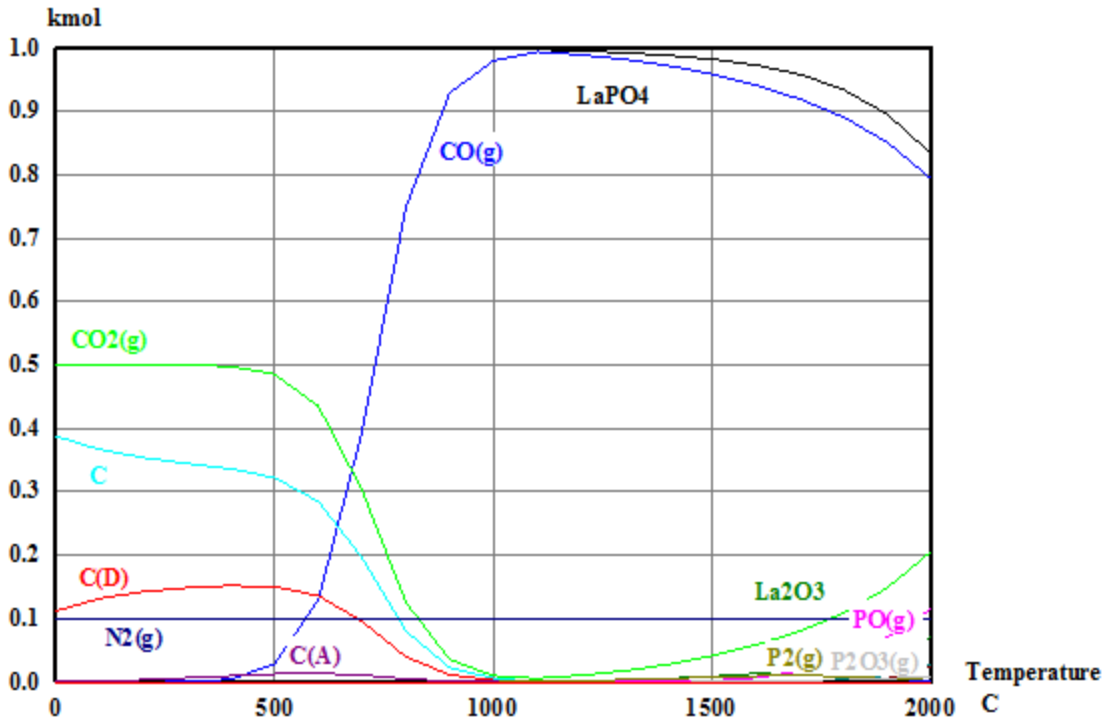
Figure 5.3: Thermal decomposition diagram of LaPO$_4$ in a reducing environment.
Input: 1 Kmole LaPO$_4$ and Kmole CO.
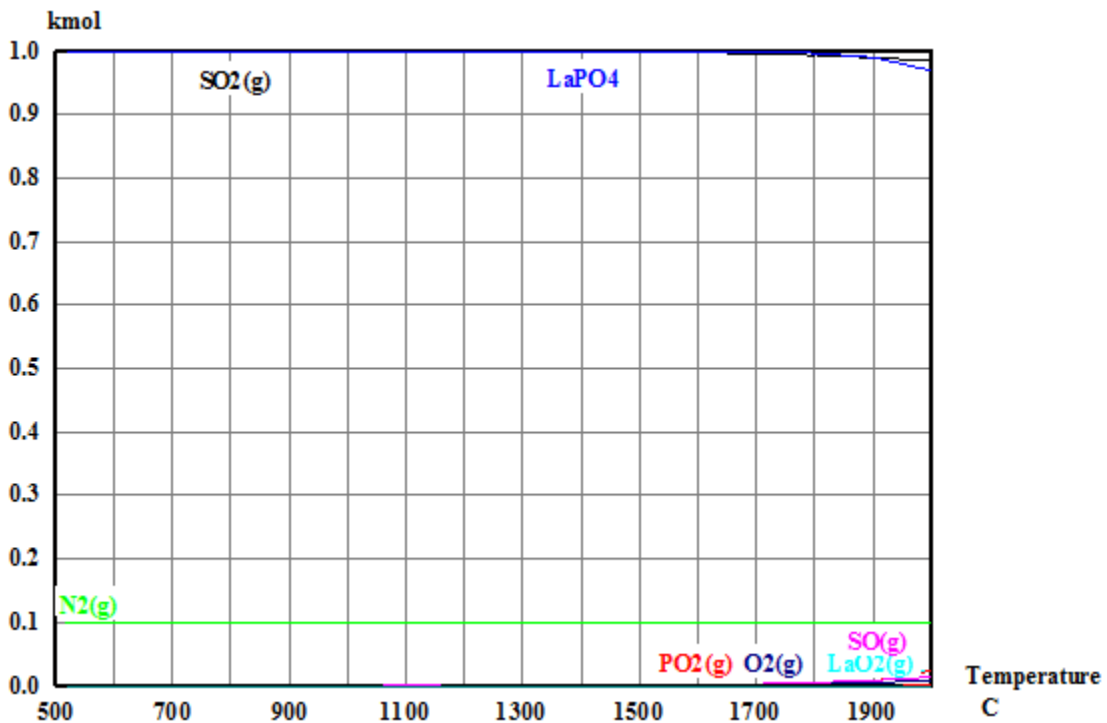
Figure 5.4: Thermal decomposition diagram of LaPO$_4$ in a sulfidizing atmosphere.
Input: 1 Kmole LaPO$_4$ and Kmole SO$_2$.
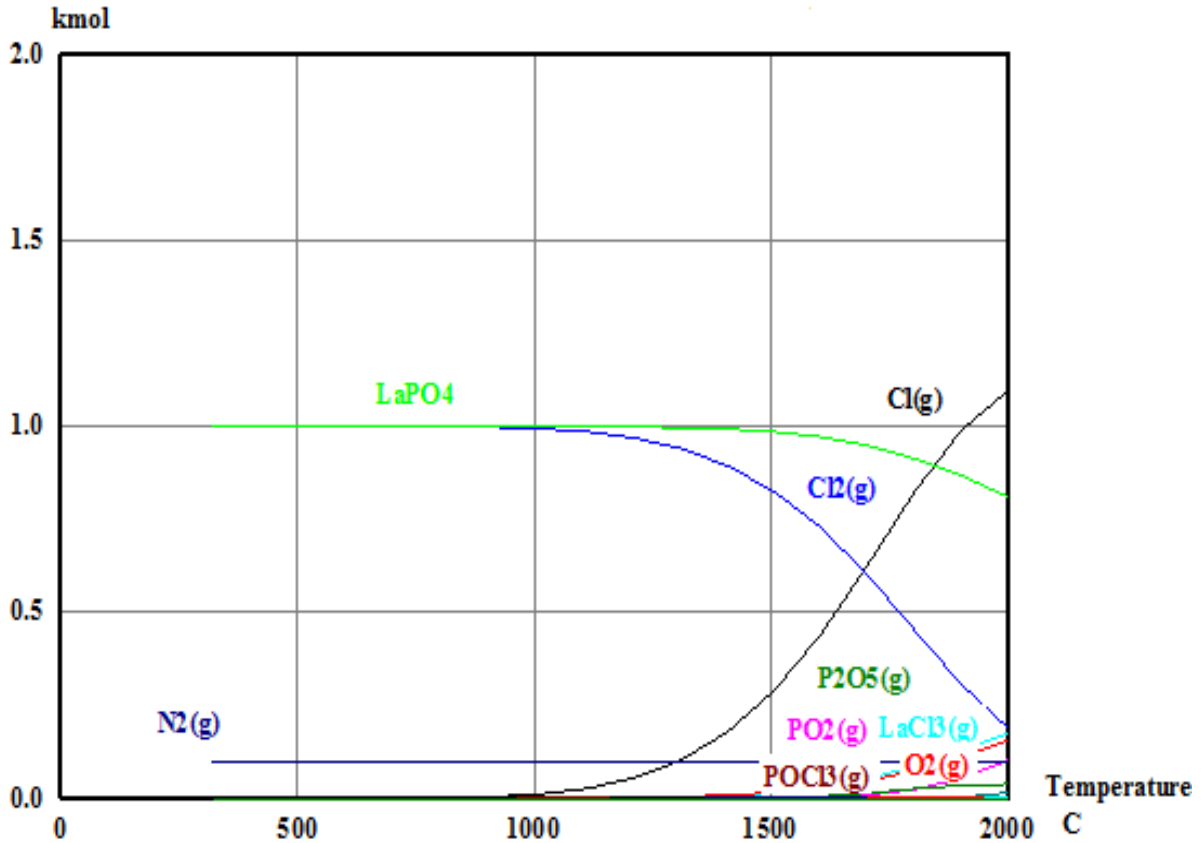
Figure 5.5: Thermal decomposition diagram of $LaPO_4$ in a chloridizing atmosphere.
Input: 1 Kmole $LaPO_4$ and Kmole Cl_2.

From the equilibrium composition diagrams, it is evident that thermal decomposition of $LaPO_4$ in air, CO, SO_2 and Cl_2 atmospheres occur at very high temperatures. This result is in agreement with the fact that the family of rare earth phosphates have been shown to possess high temperature phase stability and high melting point above 1900°C. At high temperatures ranging between 1500°C to 2000°C, less than 40% of $LaPO_4$ break down and that makes the process uneconomical for industrial application.

Thus the thermal treatment process was tested experimentally at 950°C and longer calcination time ranging from 1 hour to 8 hours to convert the rare earth phosphates to rare earth oxides. The calcine was then leached with 1.5 M HCl for the dissolution of the rare earth values. The results of the process are shown in Table 5.2 below.

Table 5.2: Leaching results after calcining the powder at 950˚C at different times.

Leaching Conditions		% Extraction			
		Calcining Conditions (950˚C)			
		Time			
		1 hr	2 hr	4 hr	8 hr
1.5 M HCl, 30 g/L, 70 ˚C, 1 hr, 200 rpm	Ce	9.62	11.43	11.07	11.21
	Tb	10.46	12.56	13.54	23.66
	La	19.09	23.74	20.74	15.42
	Eu	76.00	86.93	72.26	71.59
	Y	80.31	91.53	70.53	70.52

As expected, there was very poor extraction of Ce, Tb and La. The results show that increasing the calcination time from 2 to 8 hours doesn't improve the rare earth elements significantly. This could be due to sintering of the powder at high temperature. The extraction of Tb improves when the powder is calcined for 8 hours but the amount obtained is still low. The poor recovery of the rare earth phosphate does not justify the cost of thermal treatment at high temperature so another feasibility test was carried out at temperatures ranging between 200˚C to 850˚C and the results (Table 5.3) also show low levels of extraction of rare earth values especially Ce, Tb and La.

Table 5.3: Leaching results after calcining the powder at 550˚C and 850˚C.

Leaching Conditions		% Extraction	
		Calcining Conditions (1 hr)	
		550 ˚C	850 ˚C
1.5 M HCl, 30 g/L, 70 ˚C, 1 hr, 200 rpm	Ce	0.79	2.72
	La	2.60	5.38
	Tb	1.28	3.09
	Eu	73.85	74.32
	Y	75.80	74.79

5.3. New Process Development

A novel process for extracting the chief rare earth elements from waste fluorescent lamps has been developed. The proposed process approaches the problem of solubilizing LAP, the rare earth phosphate containing phosphor. It employs a multistage acid leach using hydrochloric acid under both mild and strong leaching conditions in addition to thermal treatment of the powder. The calcining step is in between the first and second stage leach and it is done to improve the extraction of terbium. The flowsheet for the process is shown in Figure 5.6 below.
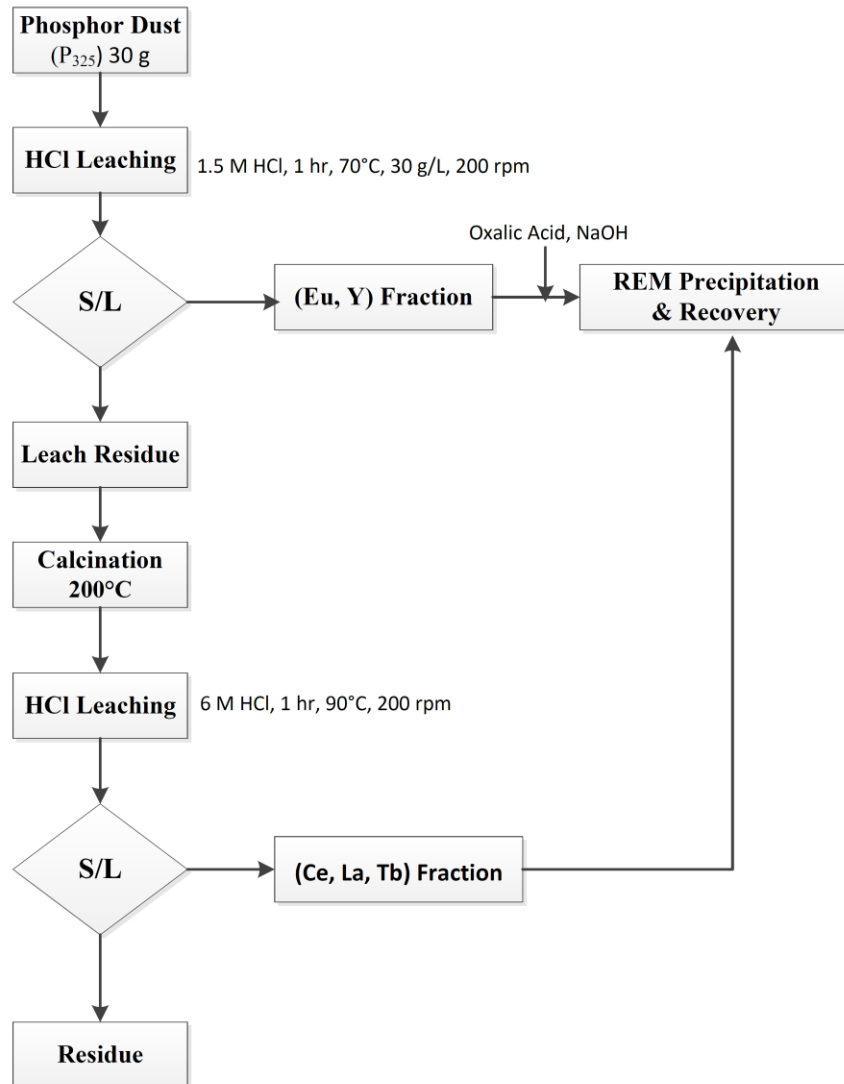
Figure 5.6: Flowsheet of new process for extraction of REEs from spent fluorescent lamps.

Europium and yttrium were removed by leaching with hydrochloric acid under the optimized conditions suggested by Takahashi et al (2003) with modifications: 1.5 M HCl, 70°C, 1 hr and 200 rpm [70]. The residue was dried and calcined for an hour to converts the rare earth phosphates into rare earth oxides. Cerium, lanthanum and terbium were then selectively solubilized by leaching with 6 M HCl or H_2SO_4. Different combinations of calcining temperatures and acid reagents were investigated to selectively extract the rare-earth values. The levels of extraction obtained after the second stage leach in the process are presented in Table 5.4 below.

Table 5.4: Leaching results after calcining the powder at different temperatures.

Leaching Conditions		% Extraction				
		Calcining Conditions (1 hr)				
		100 °C	200 °C	550 °C	800 °C	950 °C
6 M HCl, 10 g/L, 90 °C, 1 hr, 200 rpm	Ce	72.67	82.95	76.75	55.50	30.58
	La	89.66	92.62	85.56	64.95	36.67
	Tb	77.01	81.19	75.90	56.42	31.52
	Eu	0.68	0.36	0.74	3.19	1.56
	Y	0.37	0.14	0.15	0.10	0.10
6 M HNO_3, 10 g/L, 90 °C, 1 hr, 200 rpm	Ce					29.41
	La					34.87
	Tb					30.70
	Eu					1.58
	Y					0.13
6 M H_2SO_4, 10 g/L, 90 °C, 1 hr, 200 rpm	Ce					5.95
	La					6.51
	Tb					6.14
	Eu					1.78
	Y					0.17

It can be seen on Table 5.4 that at calcination temperature of 950°C, there was a significant difference in the extraction of the rare earths with respect to the acid reagent used. Hydrochloric acid and nitric acid yielded similar results although the former was higher but sulfuric acid was a poor leachate for the process at this temperature. As a result HCl was used as

the choice reagent for the other feasibility tests on this process. The extraction of Ce, La and Tb is markedly improved with this process when the powder is calcined at 200˚C. Beyond 200˚C, the level of extraction drops with increasing calcination temperature which may be due to the powder sintering at higher temperature which affects the interaction of the particles with the lixiviant.

The calcination step prior to the second stage leach is critical in achieving high dissolution of the rare earth phosphates in the powder. The extraction of terbium increased to 81.19% and so another test was performed with a longer leaching time to further enhance the extraction of terbium from the powder and the results are shown in Table 5.5 below. By increasing the leaching time to 2 hours, La extraction rises significantly from 92.62% to 98.97% but there is only a slight improvement in Ce and Tb extraction.

Table 5.5: Optimized results from calcine-leach process on the powder at 200˚C.

Leaching Conditions	% Extraction		
	Calcining Conditions (200 ˚C)		
		1 hr	2 hr
6 M HCl, 10 g/L, 90 ˚C, 1 hr, 200 rpm	Ce	82.95	86.66
	La	92.62	98.97
	Tb	81.19	84.31
	Eu	0.36	0.42
	Y	0.14	0.17

Although this process involves a selective multistage leach, there is co-dissolution of impurities with the rare earth values. As evident from Table 5.6, the bulk of the main impurities in the powder such as calcium, iron, phosphorus and zinc are removed in the first staged leach therefore creating a relatively pure rare earth concentrate for the remaining steps of the process. However, subsequent downstream purification process of the Eu and Y fraction from the first

staged leach could prove challenging and costly due to the vast amount of calcium, iron and phosphorus present in solution. Using this process, over 90% of Eu and Y is attained and 81.19% of Tb is extracted from the powder which can be recovered as REOs by a precipitation reaction.

Table 5.6: Main impurities in the leach liquor from the calcine-leach process at 200˚C.

Elements	% Extraction	
	1.5 M HCl, 70˚C, 30 g/L, 1 hr, 200 rpm	6 M HCl, 90˚C, 10 g/L, 1 hr, 200 rpm
Al	38.71	2.38
Ca	98.24	0.65
Fe	97.61	1.94
Mg	20.46	2.08
Na	17.12	6.18
P	94.29	3.68
Si	10.23	0.72
Zn	81.29	1.36

CHAPTER 6

PRECIPITATION OF RARE EARTH ELEMENTS

The separation and purification of rare earth elements (REEs) is still a matter of utmost concern and new technology or process to recover significant amount of REEs from acid solutions without compromising the purity is needed. Precipitation of rare earths from leach liquor acid solutions is the most common treatment method used today. Selective precipitation of rare earths from acid solutions was used before the industrial use of solvent extraction and ion exchange. However, selective precipitation is largely preferred due to its cost benefits and thus it has been extensively studied for industrial application. Some of research efforts on this topic include dissolution of the rare earth concentrates with ammonium carbonate and the resultant complexes treated with hydrogen peroxide for the precipitation of the corresponding peroxicarbonates [71]. Another investigative approach is the precipitation of REEs with alkaline carbonates. Firsching and Mohammadzadel determined the solubility products of rare earth carbonates [72]. Krumholz and his co-workers produced various rare earth concentrates using carbonate as precipitant, some of them for industrial application as a "rare earth carbonate", "didymium-45 carbonate", "didymium-50 carbonate", "neodymium-85 carbonate" and "yttrium-85 carbonate" [73].

Researchers have also exploited the different behavior of rare earth chlorides with oxalic acid and the differential precipitation of the corresponding rare earth oxalates. Thus oxalic acid has been used to precipitate rare earth chlorides from an acid media as rare earth oxalates, which are then fire refined by calcination to produce rare earth oxides. The proposed reaction is:

$$2 \, RE^{3+} + 3H_2C_2O_4 = RE_2 \, (C_2O_4)_3.xH_2O \, (solid) + 6H^+$$
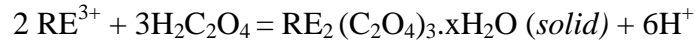
According to the reaction, the solubility decreases as the oxalic acid concentration increases and decreases as the hydrogen ion concentration in solution increases. Chung et. al. (1998) studied the solubility products of rare earth oxalates in a 0.5 M nitric acid and oxalate acid media at room temperature and they show that the solubility of rare earth oxalates decreases as nitric acid concentration decrease and oxalic acid concentration increase due to formation of rare earth oxalate complex [74]. The solubility product of the rare earth oxalates are presented in Table 6.1. Rare earth oxalates solubility in nitric acid varies from element to element.

Table 6.1: Solubility products and equilibrium constants of rare earth oxalates in 0.5 M Nitric Acid at 25 ˚C.

Element	Solubility product, K_{sp}	Equilibrium constant, β_1	Error
Y	5.1×10^{-30}	2.3×10^7	0.09
La	6.0×10^{-30}	2.2×10^7	0.078
Ce	4.0×10^{-31}	4.7×10^7	0.083
Nd	1.3×10^{-31}	4.6×10^7	0.077
Sm	4.5×10^{-32}	3.2×10^7	0.044
Eu	4.2×10^{-32}	3.3×10^7	0.061
Gd	4.25×10^{-32}	3.5×10^7	0.058
Dy	2.0×10^{-31}	4.9×10^7	0.095
Er	9.0×10^{-31}	8.0×10^7	0.055
Yb	9.5×10^{-31}	9.8×10^7	0.077

The E_h-pH diagram for Y-Cl-H_2O and La-Cl-H_2O system in Figure 6.1 – 6.2 below confirms the ease of precipitation of rare earth chlorides at room temperature at relatively low pH.
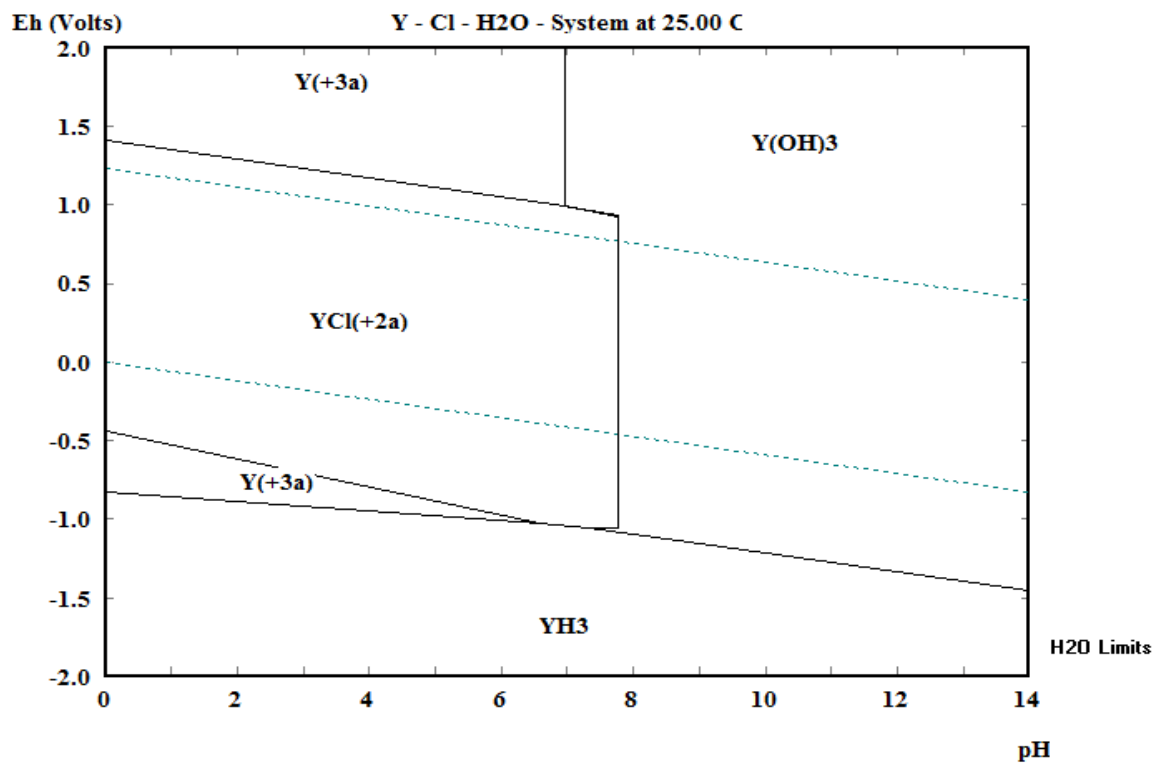
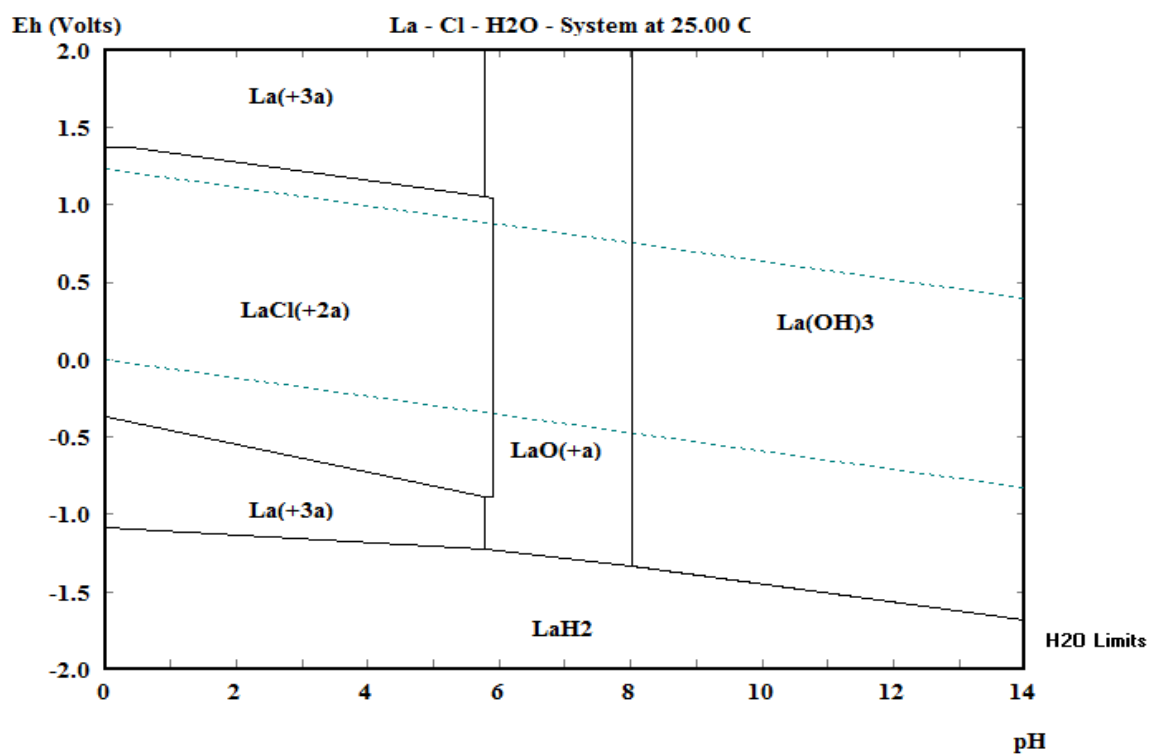**Figure 6.1:** The Eh-pH diagram for Y-Cl-H2O system at 25 ˚C.

Figure 6.2: The E_h-pH diagram for La-Cl-H_2O system at 25˚C.

Experiments were conducted with oxalic acid with different pH to evaluate the best possible precipitation conditions. The pH was adjusted with sodium hydroxide and stoichiometric amount of oxalic acid was added according to the proposed reaction for rare earth oxalate precipitation. The leach liquor used was obtained from the first and second staged leach in the newly developed process for extracting the chief rare earth elements in waste fluorescent lamps. The first stage leach liquor contains about 90% of Eu and Y and the second stage leach liquor is the Ce, La and Tb fraction which contains 82.95% of cerium, 92.62% of lanthanum and 81.19% of terbium in the powder. The REEs were precipitated from the leach liquor as rare earth oxalate and then calcined at 900˚C for 45 minutes to produce a mixed rare earth oxide (REO) powder. The results of the precipitation experiments are listed in Table 6.2.

Table 6.2: Precipitation of REE as rare earth oxalate from leach liquor at 25˚C.

Leach Liquor	Precipitation Conditions			
	pH	Time (hr)	% Precipitation of TREE	Grade of REE in mixed REO
First stage leach liquor (Eu and Y fraction)	1	2	100	39.45
	2	2	100	37.19
	3	2	100	36.23
	4	2	100	35.83
Second stage leach liquor (Ce, La and Tb fraction)	1	2	100	39.32
	2	2	100	31.00
	3	2	100	34.09
	4	2	100	31.44

As can be seen, it is relatively easier to precipitate the rare earths from an acid and oxalic acid media. All the rare earth elements are precipitated as rare earth oxalate even at pH 1. The precipitation technique used in this study was non-selective and thus there was significant co-precipitation of impurities which lead to a poor grade mixed REOs after calcination. The main impurities were calcium, aluminum, sodium, silicon, potassium, phosphorus, antimony, copper, manganese, zinc and iron. Most of the impurities were in the leach liquor which was extracted

from the powder but there were also some impurities from the precipitant media (NaOH and oxalic acid).

Further experiments should be conducted to optimize the precipitation conditions to minimize entrained impurities. However, for better results, future research effort must be also investigate reducing impurities in the leach liquor before the downstream precipitation and purification step.

CHAPTER 7

CONCLUSION

The fine particle sizes of rare earth bearing minerals make size based separation the most promising beneficiation technique in terms of grade and recovery improvements as well as process economics.

Sieving the phosphor powder to below 10 μm helps eliminate most of the silica (glass) from the feed but it is difficult and large amount of liquid filtrate is generated which have to dried by vaccum filtration at an extra operation cost. Thus although there is a slight upgrade in the REE content with fine wet sieving, the inherent operation problems and high cost associated with fine wet seiving is a major set back for industrial application. Therefore dry sieving to below 44 μm was used for further experimental evaluation of acid and base leach on the powder to extract the rare earth elements.

Using direct acid leaching or multistage leaching with mild or strong acid reagents isn't efficient for the extraction of all chief rare earths especially cerium, lanthanum and terbium. Calcining the powder under different conditions followed by leaching with a strong acid isn't effective as well. Therefore a new process was developed to improve the extraction of the chief rare earth elements. The proposed process employs a multistage acid leach using hydrochloric acid under both mild and strong leaching conditions in addition to thermal treatment of the powder. The calcining step is in between the first and second stage leach and it is done to improve the leachability of terbium. This process is effective and extracts about 90% of the europium and yttrium in the first stage leach and over 90% of lanthanum in the second stage

leach. There is also over 80% of cerium and terbium dissolution which is a significant improvement.

After dissolution of the REEs, the metals were recovered by precipitation with oxalic acid and sodium hydroxide. Precipitation of the REEs in the leach liquor was found to be relatively easy. Total recovery of the REEs was achieved even at very low pH. However, the precipitation technique was non-selective and therefore there was significant recovery of impurities in the leach liquor as well which lead to production of low purity mixed rare earth oxides after calcination.

The main challenge now is improving the dissolution of terbium from the LAP phosphor which is one of the most expensive rare earths elements today. Further research is also required to minimize co-precipitation of the impurities. A complete economic assessment of the entire process should be undertaken after the process is optimized for both dissolution and recovery of the chief rare earth metals.

CHAPTER 8

RECOMMENDATIONS FOR FUTURE RESEARCH

Significant problems still remain before finalizing a full scale recycling technique to recover REEs from spent fluorescent lamps. The following areas must be examined in greater detail to assess process viability:

1. Full phosphor characterization.

2. Prewash step to remove impurities which affect downstream processing of REEs.

3. Optimization of leaching conditions to selectively increase the solubility of terbium from LAP.

4. Optimization of precipitation techniques for impurity control to produce high purity mixed REO.

5. Quantitative evaluation of calcium, phosphor and silica flow throughout the process.

6. Efficient technique to recycle hydrochloric acid.

7. Efficient process for phosphorus and calcium recovery and recycling/disposal.

8. Life cycle analysis (LCA) of REE application in phosphors.

9. Hydrometallurgical/electrometallurgical processing for REO separation.

10. Determination of optimized flow sheet for mixed REO production.

11. Optimization of REE recovery scheme.

12. Demonstration to industry of viable technology.

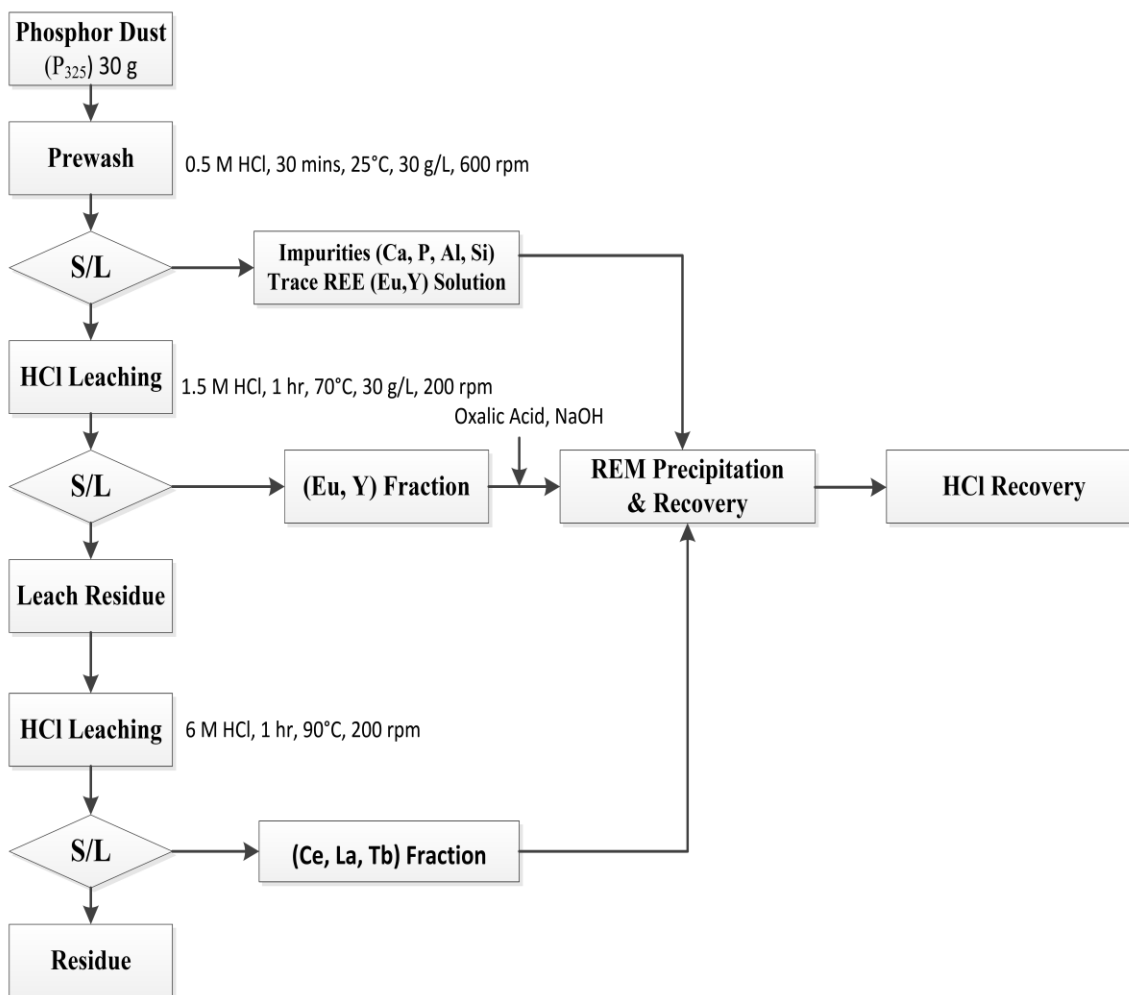A process flowsheet is hereby proposed for consideration in Figures 8.1.

Figure 8.1: Proposed flowsheet for future work.

REFERENCES CITED

[1],[4],[5],[6] Simon, W. (2010) "Breaking the Rare-Earth Monopoly", Engineering and Mining Journal, Vol 10-December.

[2]   O'Driscoll, M. (1991) An overview of rare earth minerals supply and applications. In Siribumrungsukha, B., Arrykul, S., Sanguan Sai, P., Pungrassami, T., Sikong, L., and Kooptarnon, K. (eds.), Proc. Int. Conf. Rare Earth Minerals and Minerals for Electronic Uses, Jan. 1991, Hat Yai, Thailand, pp. 409–420, Prince of Songkla University, Thailand.

[3]   Kanazawa, Y, and Kamitani, M. 2006. Rare earth minerals and resources in the world. Journal of Alloys and Compounds, 408–412, 1339–1343.

[7]   Generalic, E. "Rare Earth Elements (REE)", EniG. Periodic Table of the Elements. 28 Sep. 2013. KTF-Split.

[8],[9],[10] K.A. Gschniedner, Jr. (1992) An odyssey through rare earths. A quest for knowledge. Journal of Alloys and Compounds, 180:1-13, JAL 8000

[11]   IAMGOLD Corporation. "Rare Earths 101", April, 2012.

[12]   Kennedy, J (2009) Critical and Strategic Failure in Rare Earth Resources. A national defense and industrial policy failure.

[13],[15] Kingsnorth, D., IMCOA, "Rare Earths: Facing New Challenges in the New Decade", presented by Clinton Cox SME Annual Meeting 2010, 28 Feb – 03 March 2010, Phoenix, Arizona.

[14]   Pui-Kwan Tse, (2011) United States Geological Survey, China's Rare-Earth Industry.

[16]   Rare Earths and Critical Material Revitalization Act of 2010. H.R.6160. 22 Sep 2010.

[17]   U.S. Department of Energy. "Critical Materials Strategy", December, 2010.

[18]   Ellis, T.W., Schmidt, F.A., and Jones, L.L., "Methods and Opportunities in the Recycling of Rare Earth Based Materials", DOE Ames Lab. Report No. IS-M-796, 1994.

[19]   Zhong Xialon, Song Ning and Gong Bi., "Preparation of Mn-Zn Ferrites Powder by Waste from recycling the NdFeB Magnet Scrap", Journal of Mianyang Normal University, Vol 5, 2010.

[20]   Oakdene Hollins Research and Consulting, "Lanthanide Resources and   Alternatives", Report for Department of Transport and Department of Business,   Innovation and Skills. March 2010.

[21]   Linyan Li, Shengming Xu, Zhongjun Ju and Fang Wu. "Recovery of Ni, Co and Rare Earths from spent Ni-metal hydride batteries and preparation of spherical Ni(OH)2", Hydrometallurgy Volume 100, Issues 1-2, Page 41-46. Dec. 2009.

[22]   Bertuol, B. A., Bernardes, A.M., and Tenorio, J.A.S., "Spent NiMH batteries - The Role of Selective Precipitation in the Recovery of Valuable Metals", Journal of Power Sources, Volume 193, Issue 2, Pages 914-923, Sep. 2009.

[23]   Zhang, P., Yokoyama, T., Itabashi, O., Wakul, Y., Suzuki, T.M. and Inoue, K., "Recovery of Metal Values from Spent Nickel-Metal Hydride Rechargeable batteries", Journal of Power Sources, Volume 77, Issue 2, Pages 116-122, Feb   1999.

[24]   Mei Guangjun, Xie Kefeng and Li Gang, "Progress in Study of Spent Fluorescent Lamps' harmless disposal and resource utilization", College of Resources and Environmental Engineering, Wuhan University of Technology, China, 2007.

[25]   Buchert, M., 2010. Life Cycle Assessment (LCA) of Nickel Metal Hydride Batteries for HEV Application, Presentation at IARC, Basel (Switzerland), 4th March 2010.

[26], [41], [47] Wang, X.H., Mei, G.J., Zhao, C.L., Lei, Y.G., 2011. Recovery of rare earths from Spent Fluorescent Lamps. 5th International Conference on Bioinformatics and Biomedical Engineering, (iCBBE), Wuhan (China), 10-12 May 2011, pp. 1-4.

[26-30],[34],[40],[42],[66] Binnemans K, Jones PT, Blanpain B, Van Gerven T, Yang Y, Walton A, Buchert M, Recycling of Rare Earths: a Critical Review, Journal of Cleaner Production (2013), doi:10.1016/j.jclepro.2012.12.037.

[31],[33],[68-69] Tanmay, A. (2011). Experimental Evaluation of Recycling Rare Earth Elements from Waste Fluorescent Lamps. Unpublished master's dissertation, Colorado School of Mines, Golden, USA.

[32]   Hirajima, T., Bissombolo, A., Sasaki, K., Nakayama, K., Hirai, H., Tsunekawa, M., 2005a. Floatability of rare earth phosphors from waste fluorescent lamps. Int. J. Miner. Process. 77, 187-198.

[35]   Otsuki, A., Dodbiba, G., Shibayama, A., Sadaki, J., Mei, G.J., Fujita, T., 2008. Separation of rare earth fluorescent powders by two-liquid flotation using organic solvents. Jpn. J. Appl. Phys. 47, 5093-5099.

[36]   Otsuki, A., Dodbiba, G., Fujita, T., 2007. Separation of a mixture of rare earth fluorescent powders by two-liquid flotation using polar and non-polar organic solvents for recycling. Microprocesses and Nanotechnology 2007, Digest of Papers, pp. 236-237.

[37]   Takahashi, T., Takano, A., Saitoh, T., Nagano, N., Hirai, S., Shimakage, K., 2001. Separation and recovery of rare earth elements from phosphor sludge in processing plant of waste fluorescent lamp by pneumatic classification and sulfuric acidic leaching. Shigen to Sozai 117, 579-585.

[38]   Hirajima, T., Sasaki, K., Bissombolo, A., Hirai, H., Hamada, M., Tsunekawa, M., 2005b. Feasibility of an efficient recovery of rare earth-activated phosphors from waste fluorescent lamps through dense-medium centrifugation. Sep. Purif. Technol. 44, 197-204.

[39]   Horikawa, T. and Machida, K., 2011. Reuse and recycle processing for rare earth phosphors. Mater. Integr. 24, 37-43.

[43],[62] Takahashi, T., Tomita, K., Sakuta, Y., Takano, A., Nagano, N., 1996. Separation and recovery of rare earth elements from phosphors in waste fluorescent lamp (part II)— Separation and recovery of rare earth elements by chelate resin. In: Reports of the Hokkaido Industrial Research Institute, No. 295, pp. 37–44.

[44],[63] Takahashi, T., Takano, A., Saito, T., Nagano, N., 1999. Separation and recovery of rare earth elements from phosphors in waste fluorescent lamp (part III) -Separation and recovery of rare earth elements by multistage countercurrent extraction. In: Reports of the Hokkaido Industrial Research Institute, No. 298, pp. 37–47.

[45],[64],[70] Takahashi, T., Takano, A., Saitoh, T., Nagano, N., 2003. Separation and recovery of rare earth phosphor from phosphor sludge in waste fluorescent lamp by multistage countercurrent solvent extraction. In: Reports of the Hokkaido Industrial Research Institute, No. 302, pp. 41–48.

[46]   Takahashi, T., Takano, A., Saitoh, T., Nagano, N., Hirai, S., Shimakage, K., 2001a. J. MMIJ 117, 579.

[48]   Rabah, M.A., 2008. Recyclables recovery of europium and yttrium metals and some salts from spent fluorescent lamps. Waste Manage. 28, 318-325.

[49]   Radeke, K.H., Riedel, V., Weiss, E., Kussin, P., Gosse, I., Reimer, B., 1998. Chem. Technik 50(3), 126.

[50]   De Michelis, I., Ferella, F., Varelli, E.F., Veglio, F., 2011. Treatment of exhaust fluorescent lamps to recover yttrium: Experimental and process analyses. Waste Manage. 31, 2559-2568.

[51]   Otto, R., Wojtalewicz-Kasprzac, A., 2012. Method for recovery of rare earths from fluorescent lamps. US Patent 2012/0027651 A1.

[52]   Braconnier, J.J., Rollat, A., 2010. Process for recovery of rare earths starting from a solid mixture containing a halophosphate and a compound of one or more rare earths. Patent WO2010118967A1 (Rhodia Operations, France)

[53]   Porob, D.G., Srivastava, A.M., Nammalwar, P.K., Ramachandran, G.C., Comanzo, H.A., 2012. Rare earth recovery from fluorescent material and associated method. US Patent 8,137,645.

[54] Mio, H., Lee, J.Y., Nakagawa, T., Kano, J., Saito, F., 2001. Estimation of extraction rate of yttrium from fluorescent powder by ball milling. Mater. Trans. 42, 2460-2464.

[55] Zhang, Q., Lu, J., Saito, F., 2000. J. MMIJ 116, 137.

[56] Shimizu, R., Sawada, K., Enokida, Y., Yamamoto, I., 2005. Supercritical fluid extraction of rare earth elements from luminescent material in waste fluorescent lamps. J. Supercrit. Fluid. 33, 235-241.

[57] Yang, H.L., Wang, W., Cui, H.M., Zhang, D.L., Liu, Y., Chen, J., 2012. Recovery of rare earth elements from simulated fluorescent powder using bifunctional ionic liquid extractants (Bif-ILEs). J. Chem. Technol. Biot. 87, 198-205.

[58] Granite, E.J., H.W. Pennline, and R.A. Hargis, Novel Sorbents for Mercury Removal from Flue Gas. Industrial & Engineering Chemistry Research, 2000. 39(4): p. 1020-1029.

[59],[61] Cox, M., Solvent extraction in hydrometallurgy, in Solvent extraction principles and practice, second edition, revised and expanded, J. Rydberg, et al., Editors. 2004, Marcel Dekker, Inc.:New York.

[60] Nash, K.L., A review of the basic chemistry and recent developments in trivalent f-elements separations. Solvent Extraction and Ion Exchange, 1993. 11(4): p. 729-768.

[65] Nakamura, T., Nishihama, S., Yoshizuka, K., 2007. Solv. Extr. Res. Dev. Japan 14, 105.

[66] Mei, G.J., Rao, P., Matsuda, M., Fujita, T., 2009a. Separation of red (Y2O3: Eu3+), blue ((Sr,Ca,Ba)10(PO4)6Cl2:Eu2+) and green (LaPO4:Tb3+,Ce3+) rare earth phosphors by liquid/liquid extraction. Journal of Wuhan University of Technology-Materials Science Edition 24, 418-423.

[71] de Vasconcellos M.E., et al. Solubility behavior of rare earths with ammonium carbonate and ammonium carbonate plus ammonium hydroxide: Precipitation of their peroxicarbonates (2008) Journal of Alloys and Compounds, 451 (1-2), pp. 426-428.

[72] F.H. Firsching, J. Mohammadzadel, J. Chem. Eng. Data 31 (1986) 40–42.

[73] P. Krumholz, K. Bril, J. Behmoiras, F. Gottdenker, F.W. Lima, Proceedings of the 12th United Nations International Conference on the Peaceful Uses of Atomic Energy, vol. 28, United Nations, Geneva, September 1–13, 1958, pp. 184–195.

[74] Chung, D.Y., Kim, E.H., Lee, E.H., Yoo, J.H., 1998. Solubility of rare earth oxalate in oxalic and nitric acid media. J. Ind. Eng. Chem. 4, 277–284.